

CARNEGIE-MELLON UNIVERSITY  
MELLON INSTITUTE

NASA Research Grant NGR-39-008-014

INVESTIGATION OF STRESS CORROSION CRACKING OF TITANIUM ALLOYS

Semi-Annual Progress Report No. 4  
for the Period  
December 1, 1967 through May 31, 1968

BY

E. G. Haney and W. R. Wearmouth

MELLON INSTITUTE  
4400 Fifth Avenue  
Pittsburgh, Pennsylvania 15213

(NASA-CL-137287) INVESTIGATION OF STRESS  
CORROSION CRACKING OF TITANIUM ALLOYS  
Semiannual Progress Report No. 4, 1 Dec.  
1967 - 31 May 1968 (Mellon Inst.) 49 p

N89-70478

Unclas  
00/26 0198621

H.L.A. 6-14-68  
approved date

CARNEGIE-MELLON UNIVERSITY  
MELLON INSTITUTE

NASA Research Grant NGR-39-008-014

INVESTIGATION OF STRESS CORROSION CRACKING OF TITANIUM ALLOYS

Semi-Annual Progress Report No. 4  
for the Period  
December 1, 1967 through May 31, 1968

BY

E. G. Haney and W. R. Wearmouth

MELLON INSTITUTE  
4400 Fifth Avenue  
Pittsburgh, Pennsylvania 15213

This document may not be reproduced or published in any form in whole or in part without prior approval of the National Aeronautics and Space Administration. Since this is a semi-annual report, the information herein is tentative and subject to changes, corrections and modifications.

### ABSTRACT

A detailed investigation has been made into the failure of pure titanium and of alpha and beta titanium alloys in methanolic solutions to elucidate the mechanism of failure.

The Ti-5Al-5Sn-5Zr alpha alloy fails by a grain boundary embrittlement process which occurs independently of the applied stress. The presence of stress accelerates the process, which is considered as being largely electrochemical in nature. The time to failure of the Ti-13V-11Cr-3Al beta alloy varies linearly with the inverse of the absolute temperature. The activation energy for the process is of the same order as that determined for the diffusion of hydrogen in beta titanium. The effects of acetone, methyl ethyl ketone and acetic acid additions to methanolic solutions have been shown to exert their inhibiting effect due to a condensation reaction which produces water. The inhibiting effects of alcohols, however, cannot be explained on this basis.

### Introduction

The progress of the past six months is herewith reported. The earlier work was presented in three previous Semi-Annual Progress Reports. A summary of past accomplishments of this program is pertinent at this point.

### Summary

The major part of these investigations of the mechanism of stress corrosion cracking of titanium and its alloys has been carried out with foil specimens  $1/4'' \times 0.0025''$  to  $0.005''$  thick. Commercially produced alloys were used throughout. Alpha-, alpha+beta-, and beta-type alloys were included.

With methanol solutions containing somewhere between 0.1% and 0.5% water and at least a trace of  $\text{Cl}^-$ , experimental work has shown that all titanium alloy foil would fail within a few minutes to a few hours under a load equivalent to 75-85% of the yield strength. This includes the "purest" commercially obtainable titanium. Ti-6Al-4V alloy rod samples confirmed the rapid failure times. Sulfuric acid, bromine, and the ions  $\text{Br}^-$  and  $\text{I}^-$  were also found to effectively cause failure of titanium alloys in methanol solutions. The foil would not crack in more than 500 hours with methanol or methanol and water alone; but with only 0.0001 N NaCl added, a few ppm, failure would occur readily. When aggressive ions are present in the methanol solutions, somewhere between 1/2 to 5% water would prevent cracking, the amount depending primarily upon the quantity and

kind of ions present as well as upon the alloy and its treatment. With bromine present, more than 20% water is necessary. Cathodic protection is also possible; only small current densities produced significant increases in failure times for all alloys tested. Anodic stimulation decreased the time to failure.

There are some differences in the susceptibility to stress corrosion cracking with metallurgical variables, e.g., cold rolled foil was more resistant to attack than fully annealed foil. Nevertheless, metallurgical variables appear to be secondary as compared with the presence or absence of aggressive ions. Others<sup>1</sup> have confirmed that liquid methanol alone is not aggressive to titanium, at least for the times investigated. There are reported failures with methanol<sup>(2,3,4)</sup>, but there is no indication that the solutions were checked for possible traces of chloride contamination.

Crack propagation rates for Ti-6Al-4V alloy were measured on both rod and foil exposed to methanol-chloride solutions. The values obtained were similar and were comparable with those found by other investigators for other systems. The evidence here suggested that the cracking is a stress corrosion mechanism. Anodic stimulation hastening failure would also suggest a similar mechanism but involving electrochemical considerations. However, the investigations of titanium in methanol-chloride solutions without any applied stress showed a marked deterioration of the foil. Again, the cold rolled foil was more resistant to attack than the fully annealed foil. Such evidence suggested an intergranular corrosion mechanism or perhaps stress accelerated corrosion.

No cracking of titanium alloy occurred with ethanol-water-chloride or 2-propanol-water-chloride solutions in 500 hours without anodic stimulation. Electrode potential measurements (free corrosion potentials) confirmed that cracking would not be expected because of the nobility of the metal surface. In contrast, dimethylsulfoxide with 0.01 N HCl readily cracked titanium; but if 0.01 N NaCl was substituted for HCl, 99<sup>+</sup>% Ti foil did not break in 500 hours.

Anodic potentiostatic curves indicated excessive electrochemical activity on the metal surface when the composition of the methanol solution was such that short cracking times were observed. When enough water was added to the solution so that no cracking occurred, the maximum current density was several orders of magnitude less than the more active solutions, suggesting a passivation or inhibition. Open circuit potentials were also substantially more noble.

### Materials and Procedures

#### Materials

Two grades of commercially pure titanium and a number of commercial titanium alloys have been tested mainly in foil form, approximately 0.003" thick and 1/4" wide. The foil was obtained, having been rolled on a Sendzimir mill and sheared to 1/4"-wide strips, cut parallel with the rolling direction by automatic slitting equipment at the mill. Also, "pure" titanium in sheet form, 0.016" thick, and 3/8" diameter Ti-6Al-4V alloy rods have been tested, the results from these being found in Semi-Annual Progress Reports Nos. 2 and 3. The mill compositions of

all the alloys investigated to date are given in Table I. The tensile properties of the as-received material are found in Table II, whereas the tensile properties after laboratory heat treatments are given in Table III.

Although details of the apparatus and testing procedures have already been discussed in Semi-Annual Progress Reports Nos. 1 and 2, it is felt that a review would now be in order.

#### Heat Treatment and Tensile Testing

Heat treatment was accomplished in an electric resistance furnace after first sealing the specimens in vycor tubing under a partial pressure of helium. The tensile properties in air were obtained by testing on an Instron Testing Machine. The individual values presented in Tables II and III represent an average of at least two specimens tested. Foil specimens were tested as 1/4" strips without a reduced section.

#### Solution Preparation

Reagent grade chemicals were used throughout in the preparation of solutions, without additional purification. The water content of the methanol varied from 0.01% to 0.09% depending upon the lot. The water used was first distilled and then passed through a commercial ion exchanger; the electrical conductivity was of the order of  $6 \times 10^{-7} \text{ ohm}^{-1}/\text{cm}$ .

#### Apparatus for Testing Foil Specimens

The apparatus was designed to test the foil strips in direct tension under deadweight load conditions. The environment was contained

around the specimen in a polyethylene bottle. Figure 1 presents an overall view of the apparatus with the auxiliary equipment. To the right on the wall are 10 counters which record the times to failure of the individual specimens. The counters are activated by microswitches seen at close range in Figure 2. Also visible in Figure 2 are one of the broken specimens, about 4" long, after the polyethylene bottle has been removed, and a loaded specimen threaded through a polyethylene bottle containing the test solution. The specimens are clamped to straps on each side and the tension applied over a ball bearing on one side with a deadweight. The apparatus is also capable of testing partially immersed specimens, as shown in Figures 1 and 2, by loading the specimen in a vertical rather than horizontal position. Nearly all of the specimens investigated in the present work were totally immersed, however, and were loaded to 85% of Y.S. unless otherwise noted.

It is also possible to use an alternate immersion type of testing by means of a gravity feed system for moving the liquid in and out of the polyethylene bottle by a reciprocating motion of a reservoir of solution (see extreme right, Figure 1). In response to the timers, the exposure and immersion times of a specimen can be varied, as well as the exposure/immersion ratios. The rate of drying of alternate immersion specimens can be hastened by use of the fan directly above the testing apparatus. The gravity feed equipment can also be used for reciprocally flowing solutions.

To supplement the testing apparatus as described above, individual machines were designed whereby the specimen was loaded through a lever arm arrangement. This had several advantages in that the

machines were portable and also the smaller weight could be quickly removed as necessary, for example, in crack propagation studies.

Specimen preparation consisted of cutting a 4" length of the foil and then cleaning it with methyl-ethyl-ketone, before threading it through a 1-1/4" diameter polyethylene bottle which had two small slits cut with a razor blade. The points of emergence of the specimen from the bottle were then coated with epoxy, or in some cases with silastic 89Z-RTV adhesive sealant, to prevent leakage. Next the specimen and bottle were clamped to the removable straps of the testing apparatus using a jig which assured alignment of the straps and specimen. The foil specimen, clamp holder, and straps were then a continuous linear unit and were mounted on the frame of the testing apparatus.

#### Electrode Potential Measurements

A specimen of foil, 1/2" long, was degreased in methyl-ethyl-ketone and then screw clamped into a Teflon holder to make electrical contact with a platinum wire lead. The specimen potential was measured with respect to a silver/silver chloride reference electrode, the connection to the corrosion cell being through a KCl salt bridge and a Luggin capillary (drawn to a very fine hole) placed in a fixed position in front of the foil. The assembled holder was then immersed in the test solution, the whole assembly, including the reference electrode, being also immersed in a constant temperature bath maintained at  $30^{\circ} \pm 1^{\circ}\text{C}$ .

Values of electrode potential were measured as a function of time, zero time being taken as the moment of immersion of the specimen in

the test solution. A compensating device consisting of a micropotentiometer and a standard cell converted the potential values directly to the calomel scale, and these values were measured with a 610B Keithley electrometer. A schematic circuit diagram is shown in Figure 3(a).

#### Applied Current Measurements

For these measurements, a platinum electrode was positioned 1/2" from the foil inside the polyethylene bottle containing the sample under load. The electrical connection to the foil was made outside the bottle. Current from a filtered D.C. power source was supplied through an ammeter and a variable resistor to the platinum electrode. A microswitch and timing device were incorporated into a separate circuit to record the time to failure.

#### Potentiometric Measurements

The schematic circuit diagram for the potentiostatic measurements is shown in Figure 3(b) and includes an Anotrol Model 4700 potentiostat, a voltmeter, saturated calomel electrode bridge, and working cell. The latter has a volume of 750 ml and inlets for gas injection, reference, auxiliary and working electrodes. The auxiliary electrode is platinum. The foil specimen is mounted on a cylindrical tapered stainless steel holder with a tapered Teflon sheath holding it on and preventing access of the solution to all but a finite area of the specimen surface. The foil specimen so mounted is under an elastic bending stress. The holder arrangement is free from solution leakage, can be rapidly assembled, and provides a solderless electrical contact. The holder is mounted on a Stern-Makrides<sup>5</sup> assembly. The polarization cell is shown in detail in Figure 4.

Data were taken starting at 1 volt cathodic and proceeding to 1 volt anodic in steps of 100 mV. The values of potential set with the potentiostat were measured using an externally connected vacuum tube voltmeter that had been previously calibrated. Measurements of current were taken 5 minutes after the adjustment of potential. A magnetic stirrer was used to gently stir the test solution during a run.

### Experimental Results and Discussion

#### Investigation into the Mechanism of Failure of Ti-5Al-5Sn-5Zr in Methanolic Solutions

Foil samples of the alpha alloy, 0.003" thick, were tested in methanolic solutions using the experimental procedures as previously described. The chemical composition and tensile properties are given in Tables I and II, respectively.

Effect of Solution Composition - Earlier work in this laboratory has established that methanol solutions containing small additions of HCl or NaCl are capable of cracking the alloy when loaded to 75% Y.S. Figure 5 shows the curves obtained in solutions containing 0.01 N HCl and 0.01 N NaCl, plotting log time to failure versus log volume percentage water in methanol. It can be seen that the times to failure go through a minimum and that a sufficient water content will inhibit the cracking process, at least up to exposure times of 500 hours. The electrode potentials of unstressed specimens, measured 1 hour after immersion, are also shown in Figure 5, from which the inhibition of cracking is apparently associated, at least in part, with the increased nobility of the metal surface.

Metallographic examination of failed specimens revealed subsidiary cracking along the exposed section, the density of cracking being greater the lower the water content. However at the higher water contents, the individual cracks were found to be longer. In specimens which did not fail, no cracks were found. In all cases, the cracks were found to be mainly intergranular (Figure 6) with very little or no deformation being visible in the grains immediately adjacent to the fracture edge.

Effect of Applied Stress - By testing specimens at 25%, 45%, and 90% Y.S., a nest of curves similar to those shown in Figure 5 were plotted and are shown in Figure 7 for the methanol solutions containing HCl. As expected, the times to failure are reduced at the higher stresses as well as the percentage water needed for inhibition being slightly increased. Also, the position of the minimum remains fixed, within experimental accuracy, independently of the stress, again implying the strongly influencing nature of electrochemical phenomena, at least for crack initiation.

To further investigate the role of stress in the cracking mechanism, curves were plotted of applied stress versus log time to failure for solution compositions corresponding to the minimum and to each side of the minimum, Figure 8. It can be seen that in the region of the yield stress, where marked plastic deformation would be expected to occur, there is a sudden reduction in the time to failure. Also, the solution producing the minimum time to failure at 75% Y.S. (Figure 5) is equally effective at all applied stresses; and failure can occur under stresses as small as 10% Y.S. Therefore, it would appear that although

plastic yielding produces a marked reduction in the failure time, it is not a necessary condition for crack initiation, again suggesting the predominance of some electrochemical reaction. This suggestion is further supported by plotting curves similar to Figure 8 in which, prior to testing, the specimens were pre-plastically strained 0.5% and 2.25% (Figure 9). The shape of the curve is reproduced, independent of the prestrain the specimen received, although the stress at which there is a sudden reduction in the failure time increases slightly with the degree of prestrain.

Subsidiary tests in which the specimen was allowed to relax under stress for up to 24 hours prior to adding the solution produced similar failure times as when, more usually, the solution was added immediately after the specimen was stressed.

Crack Propagation Rates - Studies of crack propagation rates were made on the alloy in solutions corresponding to the minima and to each side of the minima in Figure 5. The detailed results are shown in Figure 10. As well as illustrating a number of interesting points, they provide a possible explanation for the occurrence of the minima in the times to failure curves with respect to water content. The main difference between the solutions containing NaCl and HCl appears to be due to the enhanced chemical reactivity of the acid solution resulting in shorter incubation times and higher crack propagation rates. The general trend in both solutions appears to be that as the water content is increased, so the crack propagation rate is gradually reduced. It must be pointed out that throughout the work, difficulty was often encountered

in solution compositions on the higher water side of the minimum, resulting in the scatter as shown in the two curves in Figure 10. However, the most important result is that the incubation times are found to go through a minimum and this effect more than off-balances the reduced propagation rate, producing a minimum in the time to failure curve. Although the reason for the occurrence of the minimum in the incubation time is obscure at this time, a possible explanation could be afforded by electrochemical considerations; the environment at the minimum being particularly favorable for crack initiation, lying between regions of general corrosion and passivation. The role of the externally applied stress may then be to concentrate and accelerate attack at the stress concentrations produced at the sites of initial electrochemical action.

Free Corrosion Tests - As previously mentioned, the cracking was characteristically brittle, and, apart from the actual cracks, metallographic examination showed no signs of any chemical attack in the form of general pitting or selective corrosion. In fact, the metal surface remained in the same condition as it was prior to immersion, i.e., bright and untarnished. To try to understand the corrosion processes occurring, the behavior of the alloy under freely corroding conditions in the absence of applied stress was studied. The effects of corrosion were ascertained from the deterioration in the tensile properties of the alloy after having been exposed to the solution for varying times. The solution compositions used were the same as those used previously to determine crack propagation rates and the results are shown in Figures 11 and 12.

From these graphs, it is evident that the acid solution is far more aggressive, particularly at the low water contents. In fact after 100 hours immersion in the  $\text{CH}_3\text{OH}/0.01 \text{ N HCl}/0.1\% \text{ H}_2\text{O}$  solution, it was impossible to handle the specimen without it disintegrating. On metallographic examination of such specimens, the grain boundaries were found to have become delineated as well-defined black lines. Due to handling, many "cracks" were found, as shown in Figure 13(a) and (b).

In specimens examined after being tested to determine residual tensile properties, "cracks" were found, much the same as in specimens stressed while immersed, i.e., intergranular, but containing a lot more associated cracking, Figure 14(a) (c.f., Figure 6). Also, whole grains were found to have fallen out (Figure 14(b)). From the metallographic evidence, it would appear that, rather than corroding, embrittling would be a far more realistic and accurate description for the effect of methanol solutions on the alloy.

Figures 11 and 12 also show that the tensile properties deteriorate uniformly as the water content is increased and the solutions corresponding to the minima in the time to failure curves do not cause the most deterioration. Therefore, it is apparent that the latter solutions have their attack greatly enhanced only when the specimens are exposed under stress.

The results have so far indicated that it is not necessary to have stress acting conjointly with corrosion to produce cracking and that cracking can be caused by applying stress after the environment has been removed. The role of the applied stress in the presence of the solution appears to be that of accelerating the electrochemical action by concentrating it at the sites of initial attack which subsequently act as stress raisers.

Effect of Applied Current - The hydrogen embrittlement of titanium alloys is well known, and, therefore, the possibility arises that this might be the reason for the failure of such alloys in methanolic solutions. This possibility is further strengthened by the observation that in specimens exposed to the solution under stress for times shorter than the incubation time, i.e., before any cracks are visible, the tensile properties have already begun to deteriorate (Table IV). The deterioration of the properties in equivalent times without stress are also shown.

Table IV  
Deterioration of Tensile Properties

Solution	Stress	Exposure Time	Elongation % in 2"	0.2% Offset Yield Strength KSI	Ultimate Tensile Strength KSI
As Received Tensile Properties:			5.7	141.9	158.1
CH <sub>3</sub> OH + 0.01 N HCl + 0.1% H <sub>2</sub> O	None	15 min.	5.2	113.5	147.0
	None	30 min.	4.6	112.1	142.0
	75% Y.S.	15 min.	3.5	118.8	142.0
	75% Y.S.	30 min.	2.0	114.9	122.5

The results also illustrate the fact that the corrosive effect of the solution is enhanced by the applied stress, before any cracks are seen to form.

The classical experiment to distinguish between an active path dissolution mechanism and hydrogen embrittlement has been to investigate the effects of externally applied anodic and cathodic currents on the times to failure of stressed specimens. In the present case it was found that a small anodic current was sufficient to markedly reduce the failure times, but that higher anodic currents did not reduce the failure times further (Figure 15). When examined metallographically, the specimens were found to contain a high density of mainly intergranular cracks, both edge and within the foil. Cathodic current densities up to  $6.5 \text{ mA/in}^2$  prevented failure in both the solutions containing HCl and NaCl. Therefore, it would appear that the alloy failure results from an anodic dissolution mechanism rather than a hydrogen embrittlement mechanism.

It is of interest that in ethanol containing solutions, no failure resulted up to 500 hours exposure at 75% Y.S. However, the application of a small anodic current was found to cause failure in times comparable to those in the methanolic solutions under equivalent anodic currents (Figure 15).

The necessity for the presence of methanol in promoting grain boundary embrittlement was shown by testing the alloy under stress in a 3.5% NaCl aqueous solution. In the absence of applied currents, no failure occurred up to 500 hours exposure at 75% Y.S. However when anodic currents were applied, the specimens failed, the times to failure steadily decreasing as the anodic current was increased (Figure 15). It is evident that the shape of the curve is totally different from those

for the methanolic solutions. The failed specimens were found to contain large edge pits, and invariably the failure was found to have propagated from such a pit. When examined metallographically, there was found to be a complete absence of cracking and no indication of grain boundary embrittlement. It is concluded that the mechanism of failure was mainly due to overload conditions as a result of the reduction of the cross-sectional area by the pitting.

Effect of Heat Treatment - To further investigate the mechanism of failure, the alloy was heat treated in a helium atmosphere at temperatures between 1000°F and 1600°F. Table III shows the heat treatments and the resultant tensile properties.

Curves of applied stress versus time to failure for a given solution (Figure 16) were found to be similar in shape to the curves for the as-received material, the marked decrease in the failure times occurring at lower stresses probably because of the lower yield strengths of the heat-treated material. However, it is worthy of mention that for a given stress the times to failure do not decrease uniformly with increasing heat treatment temperatures but that the 1600°F and 1010°F heat treated specimens are more susceptible than the 1400°F heat treated specimens.

Using the same heat treatments, the variation in failure times with water content of the  $\text{CH}_3\text{OH}/0.01 \text{ N HCl}$  solution was studied and the results are shown in Figure 17. The relative susceptibilities to cracking are seen to be dependent upon the water content of the methanol as well as upon the heat treatment. Also, 3% water is needed to inhibit cracking in the 1010°F heat treated specimens, whereas 1.5% water is sufficient for

all the other states of heat treatment. The reason for the marked susceptibility induced by the 1010°F heat treatment is not understood at present.

At the present time, it would appear that failure of the Ti-5Al-5Sn-5Zr alloy occurs by a grain boundary embrittling process which takes place in the presence or absence of an externally applied stress. If stress is applied, the embrittling process is accelerated. The effects of externally applied anodic and cathodic currents would seem to imply that the embrittlement is not due to hydrogen. The minima in the times to failure curves as a function of water content are related mainly to electrochemical factors with respect to the incubation period for crack initiation. A sufficient water content will inhibit cracking, most probably due to the passivation of the metal surface. Although the chemical reactions which are responsible for the embrittling process are not known, it is doubtful whether the phenomenon is one of stress corrosion cracking in the classical sense; and this would further lend credibility to the failure of "pure" titanium in methanolic solutions, as generally "pure" metals are not thought to be susceptible to stress corrosion cracking.

#### Effect of Organic Liquid Additions to Methanol

An extensive investigation was made with 99<sup>+</sup>% Ti foil (S206) comparing the effects of adding water or certain organic liquids to methanol. The chloride ion was added as HCl in preference to NaCl because the solubility of NaCl in most of the organics of interest is limited. Figure 18 presents the results for the water addition at three

levels of HCl content. The higher the HCl content, the more water was necessary to stop the cracking and the deeper was the minimum in the time to failure curve. This is similar to what has been found for other alloy foils and noted in Semi-Annual Reports Nos. 2 and 3. The water carry-over from the HCl additions limits the investigations of lower water contents.

The time to failure and corresponding electrode potential measurements are shown in Figure 19 as a function of the organic liquid added to the methanol. The data points for the alcohols and carbon tetrachloride fell into a fairly narrow range up to at least 60% of the addition and are represented as a band. The alcohols were not as effective in preventing cracking of the foil as acetone, methyl ethyl ketone (MEK), or acetic acid. The electrode potential measurements would predict such behavior. In no instance did any cracking occur within 500 hours without at least a few percent of methanol present.

Condensation reactions can occur in ketones in the presence of HCl to form water as one of the products<sup>6</sup>. Other reactions might also be possible so that the water content of some of the solutions might not be less than about 0.1% as anticipated from the reagents used in making the solutions. The table below lists the methanol solutions analyzed for water by the Karl Fischer method. The samples were not in contact with titanium. The percentages refer to volume:

	<u>% H<sub>2</sub>O</u>
Methanol + 10% Acetone + 0.01 N HCl	1.18
Methanol + 10% Acetone + 0.01 N NaCl	.088
Methanol + 10% MEK + 0.01 N HCl	.485
Methanol + 10% MEK + 0.01 N NaCl	.113
Methanol + 10% Acetic Acid + 0.01 N HCl	1.08
Methanol + 10% Acetic Acid + 0.01 N NaCl	.763
Methanol + 0.5% Acetic Acid + 0.01 N HCl	.25
Methanol + 20% n-Octyl Alcohol + 0.01 N HCl	.109
Methanol + 90% n-Octyl Alcohol + 0.01 N HCl	.092

The water content alone can account for the apparent inhibiting effect of acetic acid, acetone, and MEK as shown in Figure 19 and comparing with Figure 18. Additional proof of the effect of water can be seen in Figure 20, which compared HCl with NaCl as additions. Note the water content differences for 10% MEK in the table. However, do alcohols prevent cracking by any reactions involving water. It seems doubtful, because the amount of water in n-octyl alcohol is about the same low water at 20% and 90% (see table). At the 20% n-octyl alcohol level, the foil was easily cracked; but the foil did not crack in 500 hours at the 90% level. The curves for 2-propanol have similar shapes whether NaCl or HCl was used (see Figure 21), again indicating no reactions involving water.

### Effect of Temperature

The dependence of the time to failure on the testing temperature was studied from 50°C to -45°C in methanol-water-chloride solutions for the Ti-13V-11Cr-3Al foil. The specimens were stressed to 75% of their yield strength at the testing temperature. The minimum in the curves occurred over a more restricted range of water contents as the temperature was decreased without much shift in position with respect to water; see Figure 22. If the shortest time to failure for each temperature is plotted against the reciprocal of the absolute temperature, a straight line is obtained; see Figure 23. An activation energy of 6.5 kcal/mole was calculated for this thermally activated process from the usual Arrhenius treatment of such data. The value is rather low for a chemical process but does correspond to the diffusion of hydrogen in beta titanium, 6.64 kcal/mole, as determined by Wasilewski and Kehl<sup>7</sup>. Additional work is currently in progress on the 99.5% Ti alloy to see if the activation energy obtained would correspond with the 12.8 kcal/mole value obtained for alpha titanium for hydrogen diffusion<sup>7</sup>.

### Conclusions

The following conclusions are based on the work accomplished in the period December, 1967 through May, 1968.

1. Failure of the Ti-5Al-5Sn-5Zr alpha alloy in methanolic solutions occurs by a grain boundary embrittling process which takes place in the presence or absence of an externally applied stress. If stress is present, the embrittling process is accelerated.

2. The minimum in the time to failure curve as a function of water content is related mainly to electrochemical factors with respect to the incubation period for crack initiation.

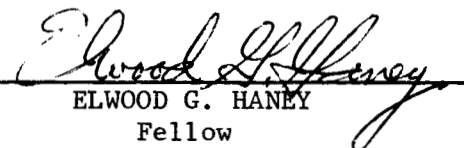
3. At this time, the chemical reactions that are responsible for the grain boundary embrittlement process are not known. It is doubtful whether the phenomenon is one of stress corrosion cracking in the classical sense, and this would further lend credibility to the failure of pure titanium in methanolic solutions, as generally "pure" metals are not thought to be susceptible to stress corrosion cracking.

4. The cracking of Ti-13V-11Cr-3Al foil in methanol-water-chloride solutions was temperature dependent and an activation energy of 6.5 kcal/mole was obtained. This value corresponds to that determined for the diffusion of hydrogen in beta titanium.

5. The addition of other alcohols or  $\text{CCl}_4$  to methanol was found to be ineffective in preventing cracking of 99<sup>+</sup>% Ti foil in methanol-chloride solutions unless additions of 80 to 95% were made. The effectiveness of acetone, MEK and acetic acid depended upon whether NaCl or HCl was added. With a NaCl addition, acetone and MEK were no more effective than the alcohols. With a HCl addition, condensation reactions in the solution produced water which thus acted as the inhibitor.

EGH:nm

R: 6-12-1968  
T: 6-13-1968

  
ELWOOD G. HANEY  
Fellow

### References

1. J. R. Ambrose and J. Kruger, Corrosion Science, 1968, 8, 119.
2. R. L. Johnston, R. E. Johnson, G. M. Ecord and W. L. Castner, NASA Technical Note NASA TN D-3868, February 1967.
3. D. A. Meyn, E. P. Dahlberg and C. D. Beachem, NRL Memorandum Report 1744, January 1967.
4. T. R. Beck, Boeing Scientific Research Laboratories, Quarterly Progress Report No. 2, December 1966.
5. M. Stern and A. C. Makrides, J. Electrochem. Soc., 1960, 107, 782.
6. Fieser and Fieser, Advanced Organic Chemistry, Reinhold Company, New York City, 1961, p. 458.
7. R. J. Wasilewski and G. L. Kehl, Metallurgia, Manchr., 1954, 50, 225.

TABLE I  
Chemical Composition, Weight Percent

Alloy	Designation	Al	V	Mo	Zr	Sn	Cr	Pd	Fe	O	C	N	H	H <sup>†</sup> ppm	Alloy No.
99.5 Ti (sheet)	MST-30													104	S-201
99.5 Ti (foil)	Ti-35A								.07	.07	.023	.010	.004	42	S-210
99.0 Ti (foil)	Ti-75A								.14	.38(max.)	.025	.016	.005	74	S-187
99.0 Ti (foil)	Ti-75A													52	S-206
Ti-0.2 Pd (foil)	Ti-0.2Pd							.20						85	S-203
6Al-4V (foil)	Ti-6Al-4V	6.0	4.0						.21	.134	.02	.01	.001	269	S-174
6Al-4V (foil)	Ti-6Al-4V	6.4	4.0						.08		.02	.008	.0125	84	S-211
6Al-4V (rod)	MST-6Al-4V	6.3	4.2						.24	.102	.02	.007	.006		S-193
5Al-5Sn-5Zr (foil)	Ti-5Al-5Sn-5Zr	5.3		5.3	5.1				.05	.10	.025	.011	.006	130	S-197
6Al-2Sn-4Zr-2Mo (foil)	Ti-6Al-2Sn-4Zr-2Mo	6.0		2.0	3.9	2.1			.06	.10	.025	.012	.010	37	S-204
13V-11Cr-3Al (foil)	Ti-13V-11Cr-3Al	3*	13*				11*		.08		.016	.017	.007	46	S-135
13V-11Cr-3Al (foil)	Ti-13V-11Cr-3Al	3.2	13.8				10.6		.21	.12	.04	.03	.0132	160	S-212

\* Nominal

† Hydrogen measurements made on foil or sheet, other determinations made at mill.

TABLE II

## Tensile Properties of Titanium Alloys As-Received

Alloy	Condition	0.2% Offset Yield Strength (KSI)	Ultimate Tensile Strength (KSI)	Elongation % in 4 IN	Alloy No.
99.5 Ti (.016" sheet)	C.R.*	98.5	119.3	6.2	S-201
99.5 Ti (.0035" foil)	C.R.*	103.6	127.2	6.9	S-210
99.0 Ti (.0055" foil)	C.R.*	124.5	137.8	6.2	S-187
99.0 Ti (.0033" foil)	C.R.*	129.3	142.2	7.2	S-206
Ti-0.20Pd (.0033" foil)	C.R.*	58.8	72.9	23.0	S-203
Ti-6Al-4V (3/8" D rod)	Hot rolled and A <sup>†</sup>	143.5	144.0	8.2**	S-193
Ti-6Al-4V (.0028" foil)	C.R.* and A <sup>†</sup>	131.7	170.5	12.8	S-174
Ti-6Al-4V (.0040" foil)	C.R.* and A <sup>†</sup>	116.3	148.9	9.1	S-211
Ti-5Al-5Sn-5Zr (.0030" foil)	C.R.* and Partially A <sup>†</sup>	138.7	156.4	3.9	S-197
Ti-6Al-2Sn-4Zr-2Mo (.0031" foil)	C.R.*	147.3	190.4	5.1	S-204
Ti-13V-11Cr-3Al (.0025" foil)	C.R.*	172.8	181.6	3.8	S-135
Ti-13V-11Cr-3Al (.0037" foil)	C.R.* and A <sup>†</sup>	134.6	135.1	25.9	S-212

\* Cold rolled

† Annealed

\*\* (in 1.25 IN)

TABLE III

Tensile Properties of Titanium Alloys after Heat Treatment

Alloy and original No.*	Treatment	0.2% Offset		Ultimate Tensile Strength (KSI)	Elongation % in 4 IN	New No.
		Yield Strength (KSI)	Strength (KSI)			
99.5 Ti (S-201)	Annealed 2 hr. at 1300°F	31.7	50.6	31.0		S-202
99.5 Ti (S-210)	Annealed 1 hr. at 1300°F	34.9	47.7	28.8 (in 2 IN)		S-217
99.0 Ti (S-187)	Annealed 2 hr. at 1025°F	80.8	90.0	21.5		S-199
99.0 Ti (S-187)	Annealed 2 hr. at 1300°F	81.6	100.4	28.0		S-200
99.0 Ti (S-206)	Annealed 2 hr. at 1025°F	74.5	90.8	29.9		S-208
Ti-5Al-5Sn-5Zr (S-197)	Annealed 2 hr. at 1010°F	136.8	144.5	8.0 (in 2 IN)		S-214
Ti-5Al-5Sn-5Zr (S-197)	Annealed 2 hr. at 1400°F	120.0	127.8	14.3 (in 2 IN)		S-215
Ti-5Al-5Sn-5Zr (S-197)	Annealed 30 min. at 1600°F	120.0	124.0	11.3 (in 2 IN)		S-216
Ti-13V-11Cr-3Al (S-135)	Solution treated at 1400°F, C.W.Q. + 24 hr. at 900°F.	165.6	175.2	4.9		S-168

\* See Table I and II

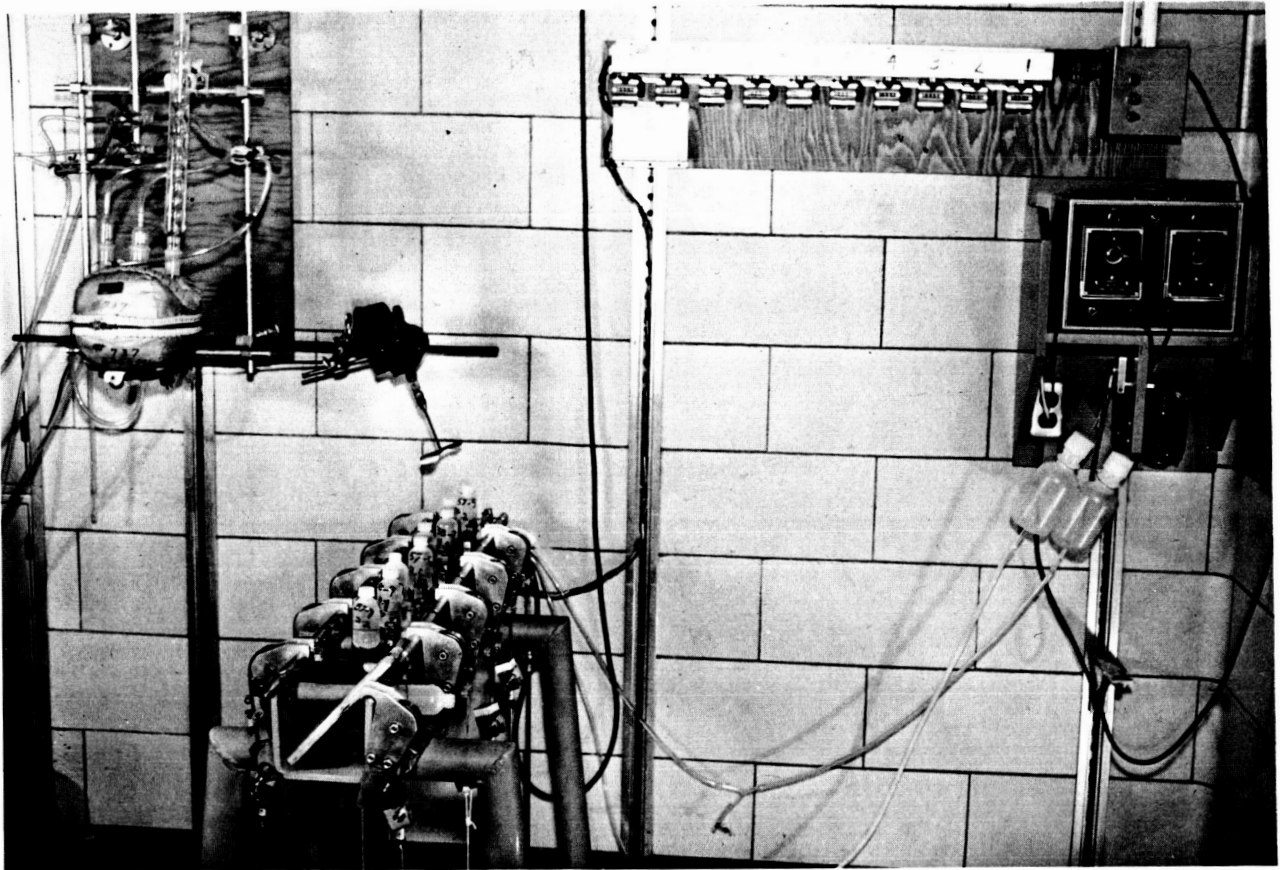
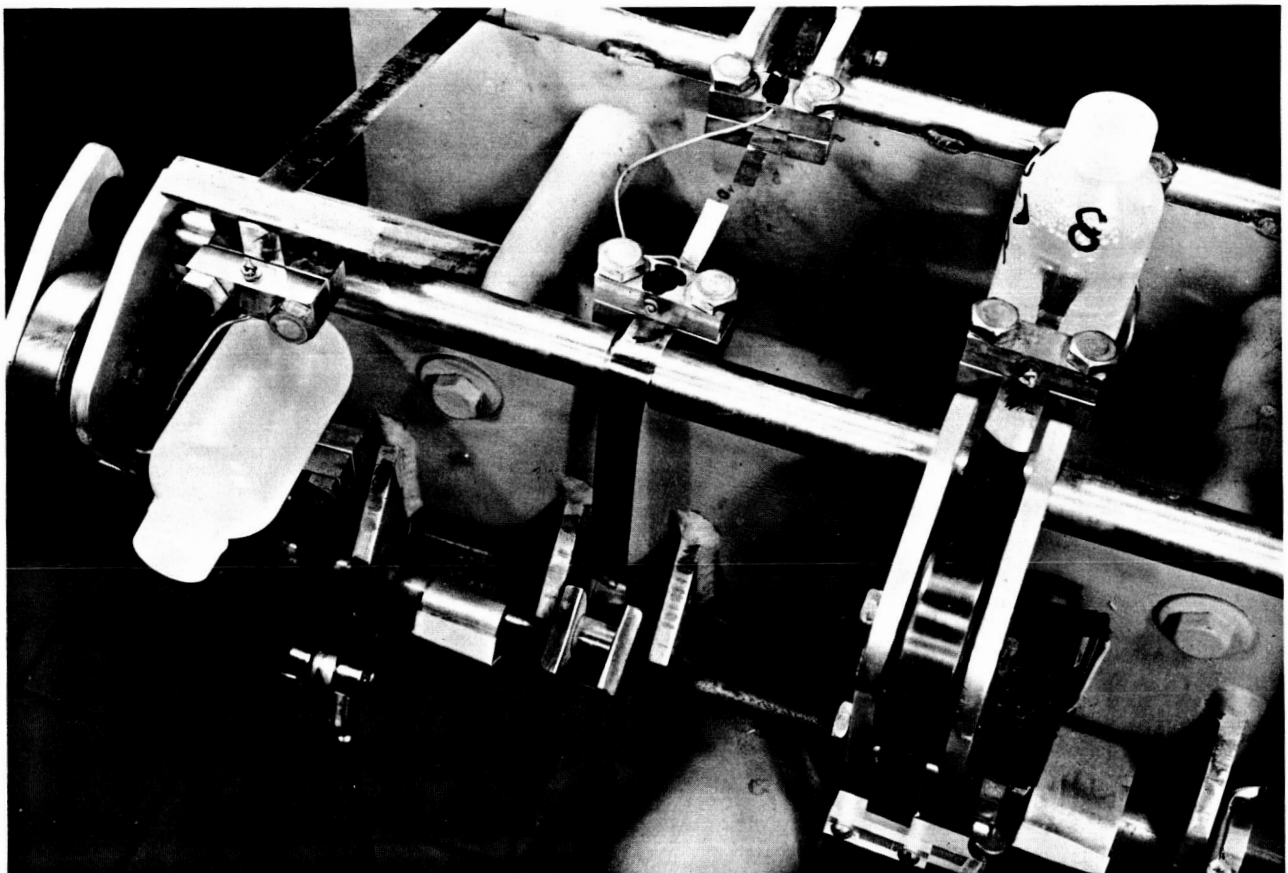


Figure 1--Apparatus for Stress Corrosion Testing of Foil at Constant Stress and its Auxiliary Equipment.

Figure 2--A closer view of stress corrosion testing apparatus showing partial immersion set-up (left), a cracked specimen with bottle removed (center), and a stagnant immersion test in progress (right).



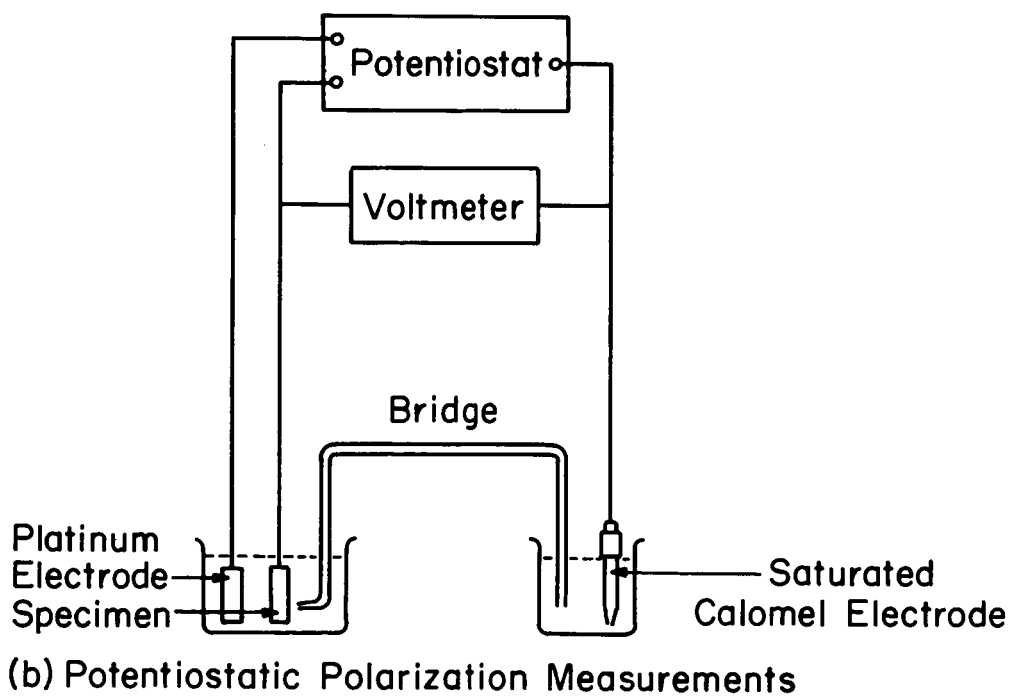
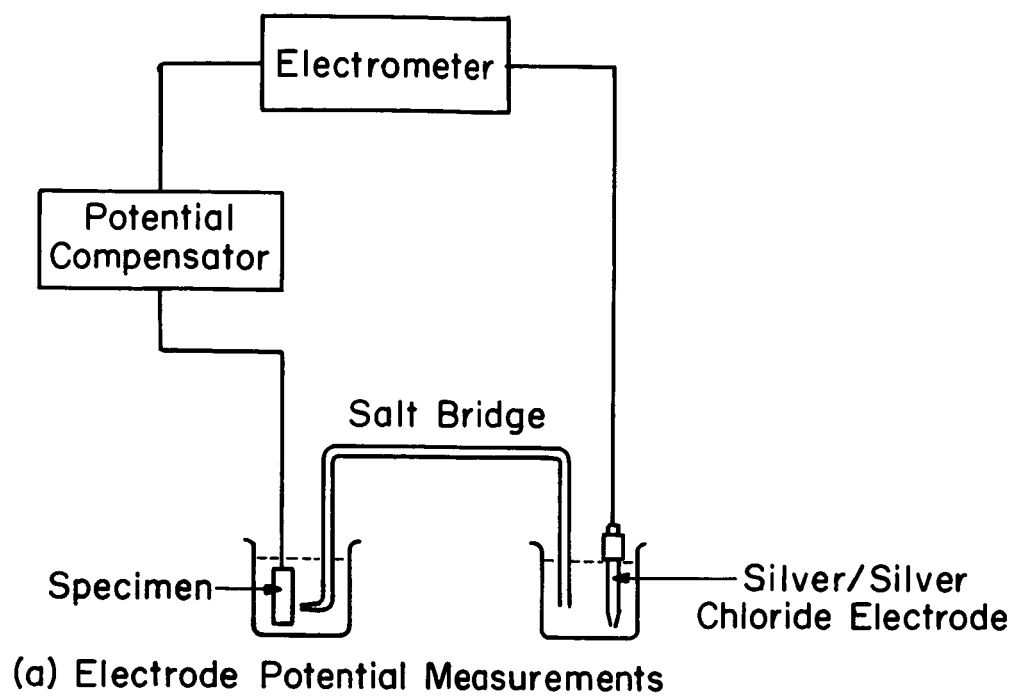


Figure 3. Schematic Circuit Diagrams

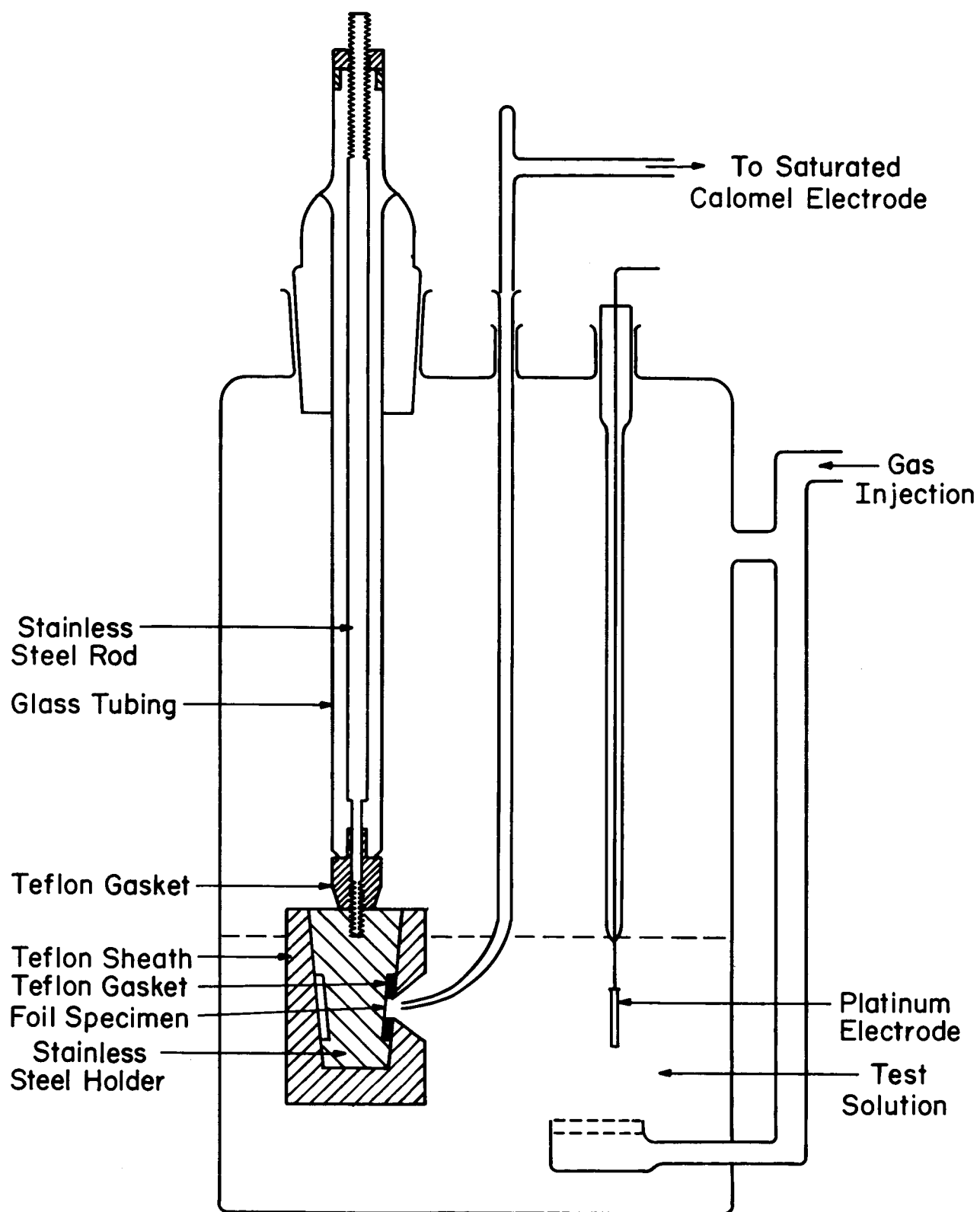


Figure 4. Polarization Cell

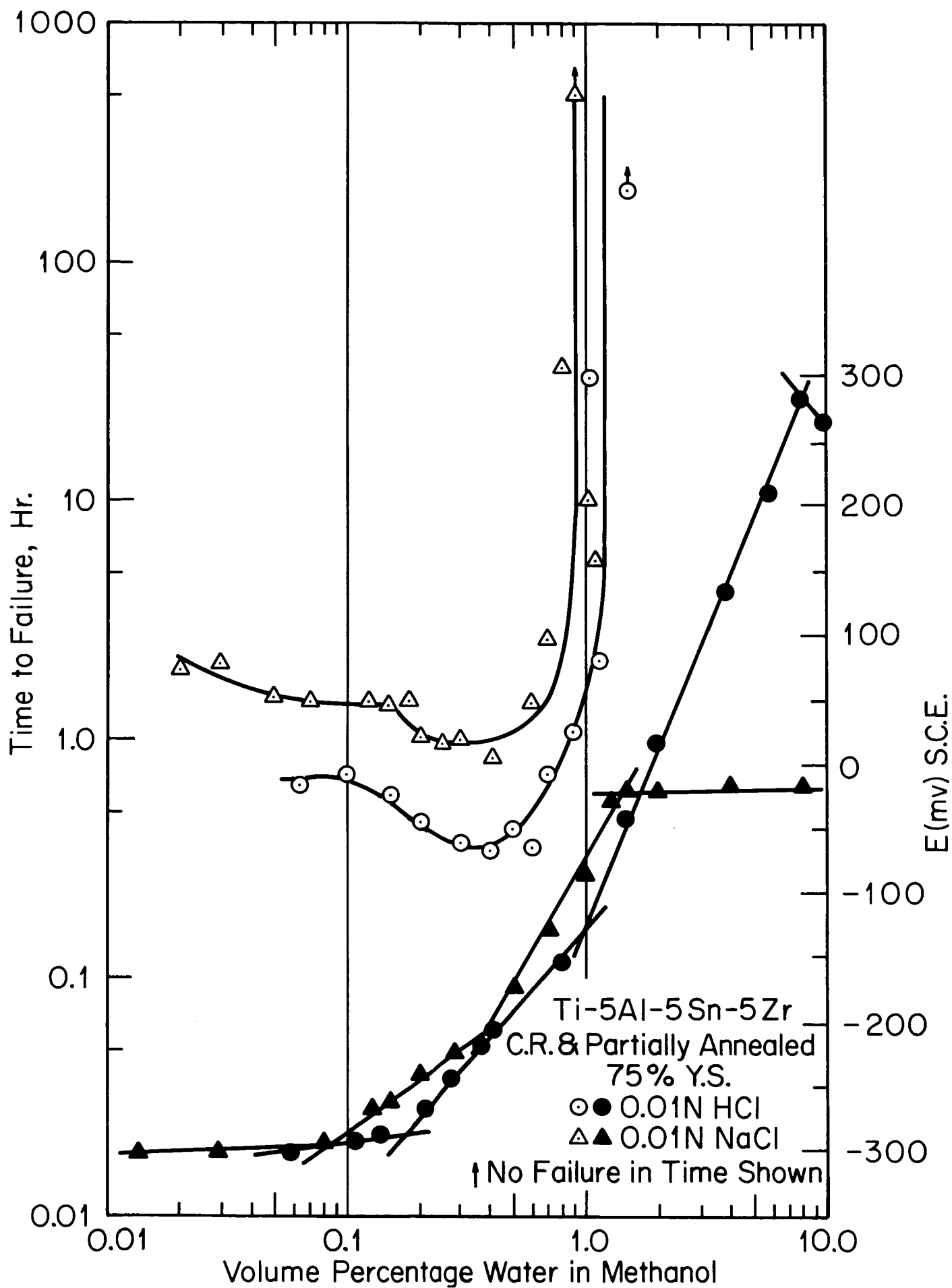


Figure 5 Comparison of time to failure with one-hour electrode potential value.



Figure 6 Intergranular crack in Ti-5Al-5Sn-5Zr, tested at  
75% Y.S. in  $\text{CH}_3\text{OH} + 0.01\text{NNaCl} + 0.25\% \text{H}_2\text{O}$ .

Etched 250X

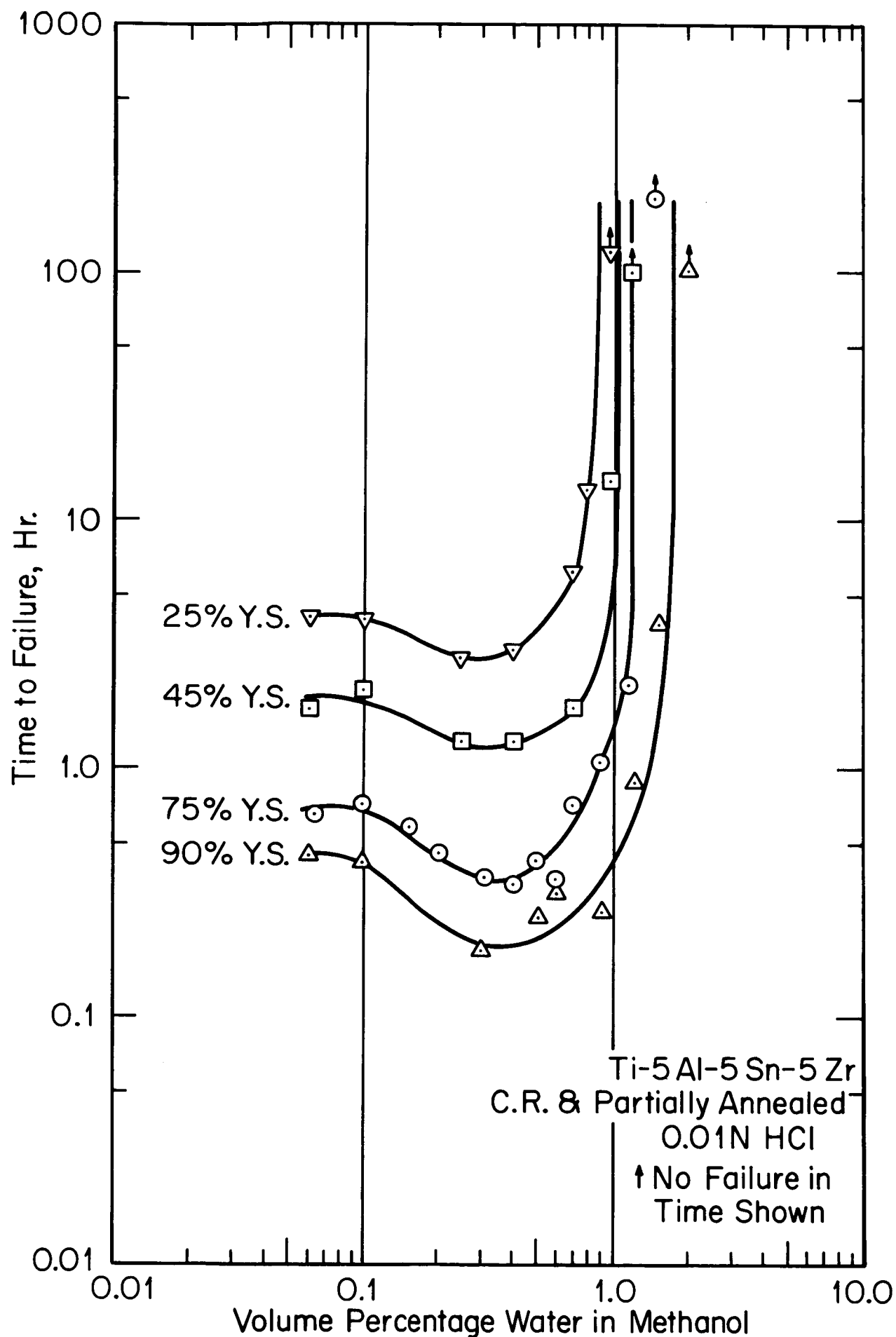


Figure 7 Effect of stress level and solution composition on time to failure.

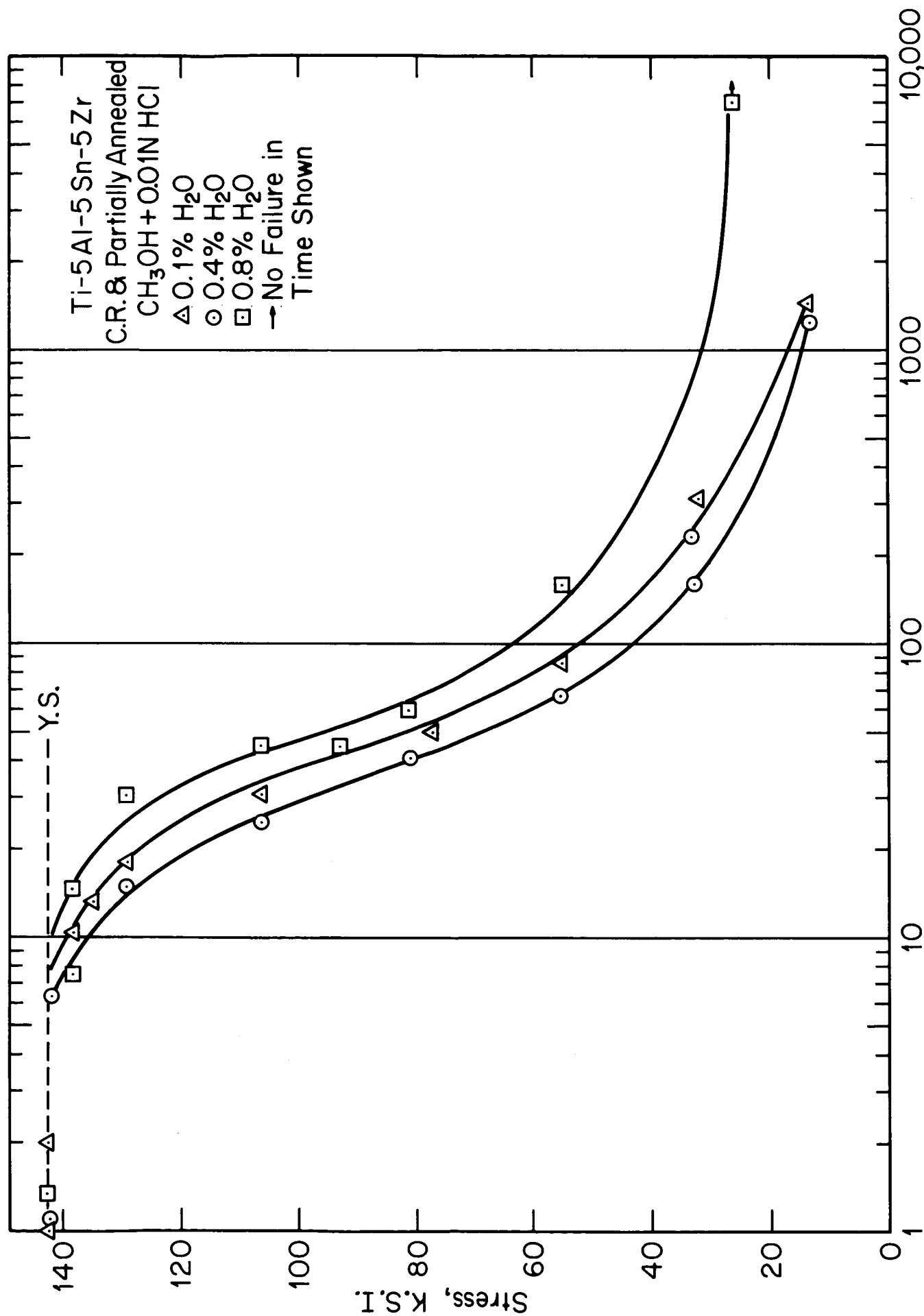


Figure 8 Effect of applied stress on time to failure.

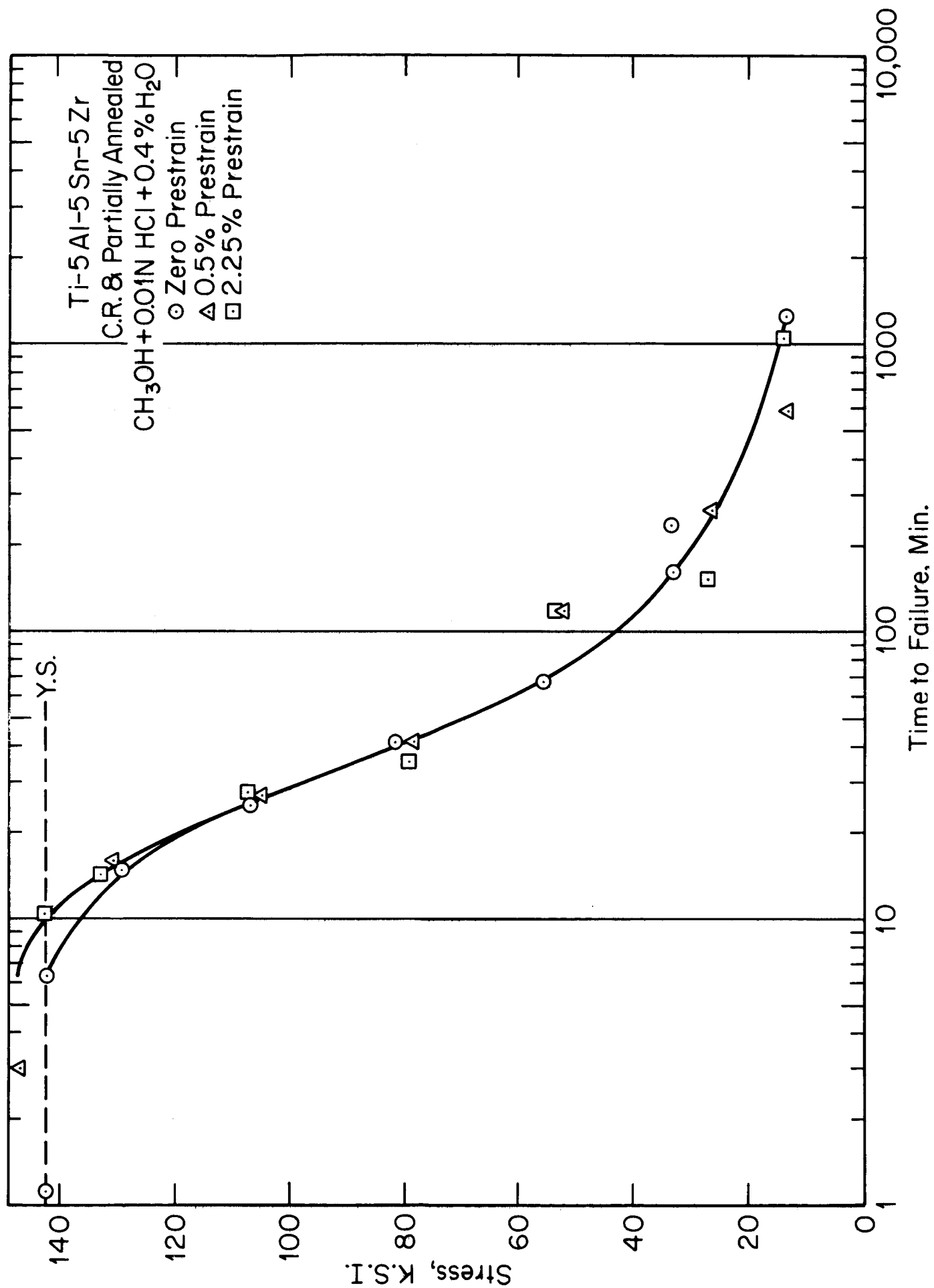


Figure 9 Effect of prestrain on time to failure.

Ti-5Al-5Sn-5Zr  
C.R. & Partially Annealed 75%Y.S.

CH<sub>3</sub>OH + 0.01N NaCl

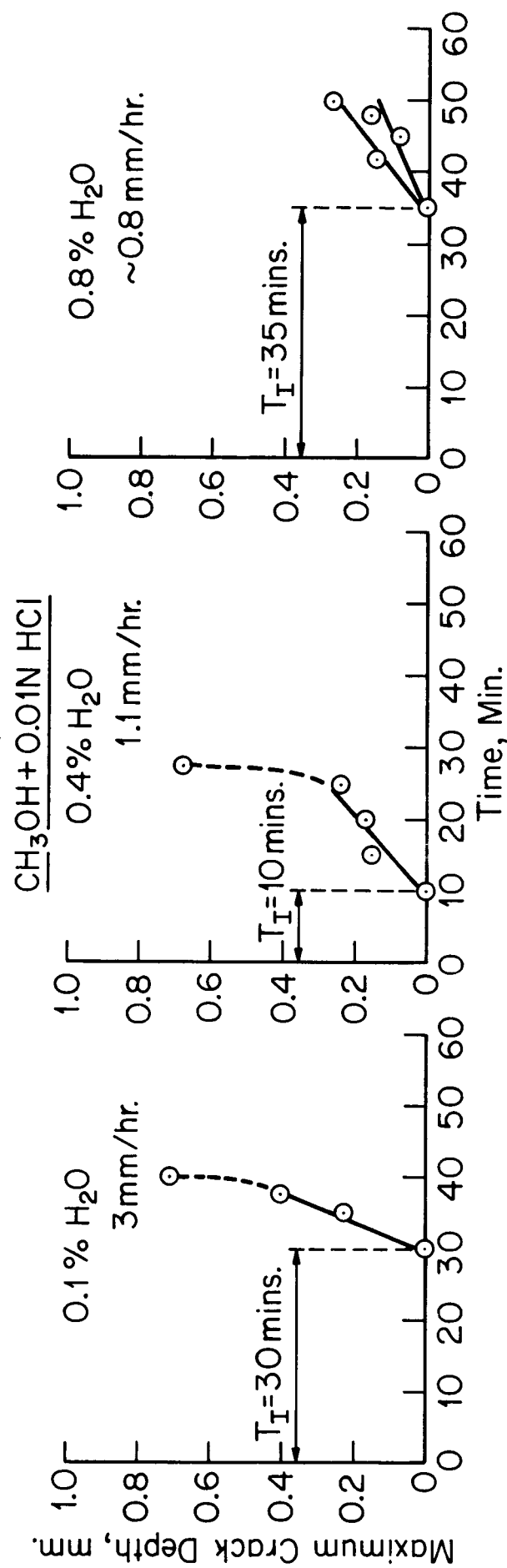
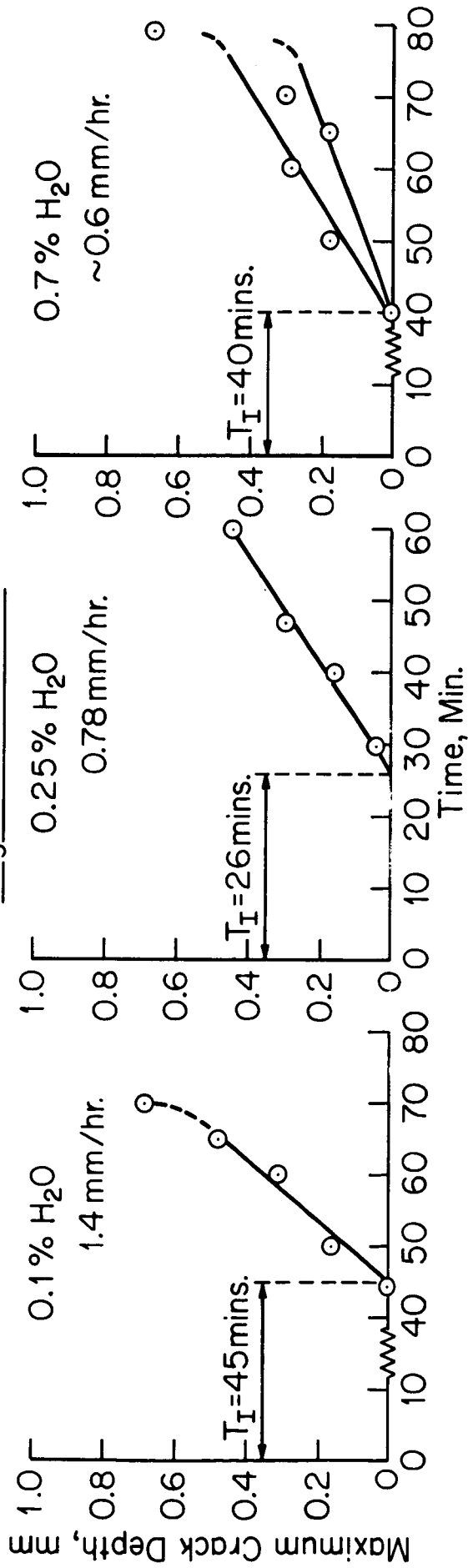


Figure 10 Effect of solution composition on crack propagation rates.

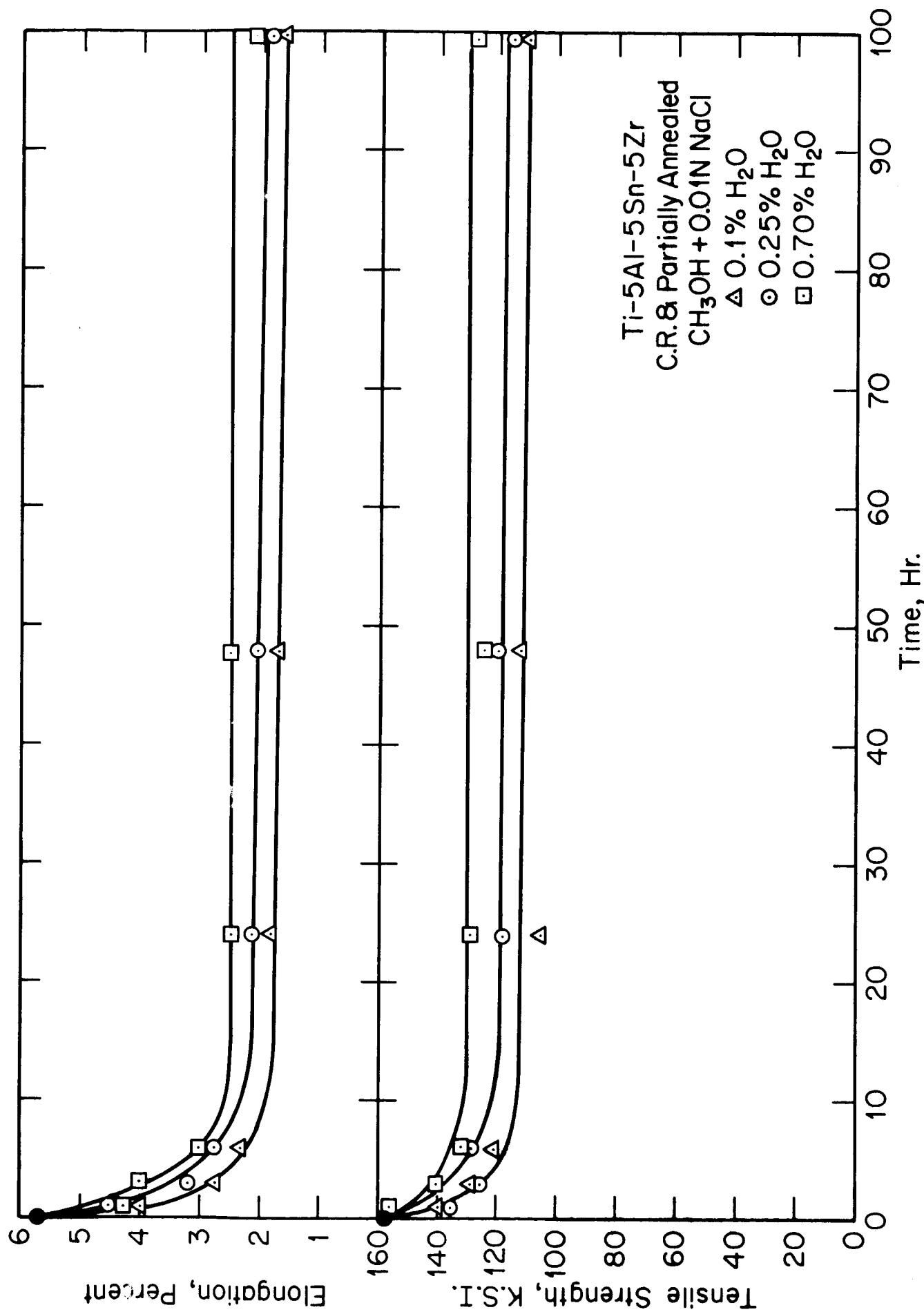


Figure 11 Deterioration of tensile properties in absence of stress.

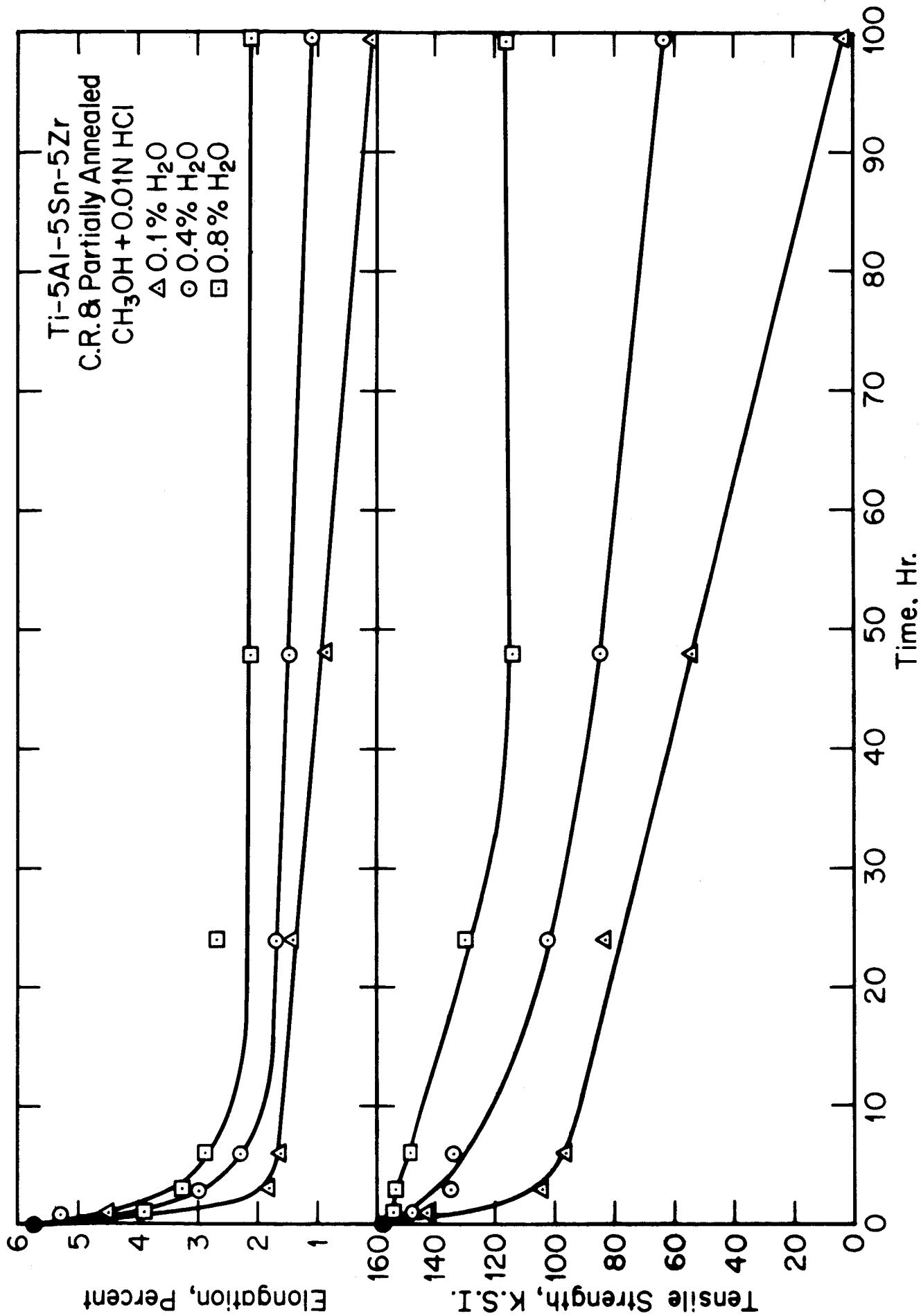
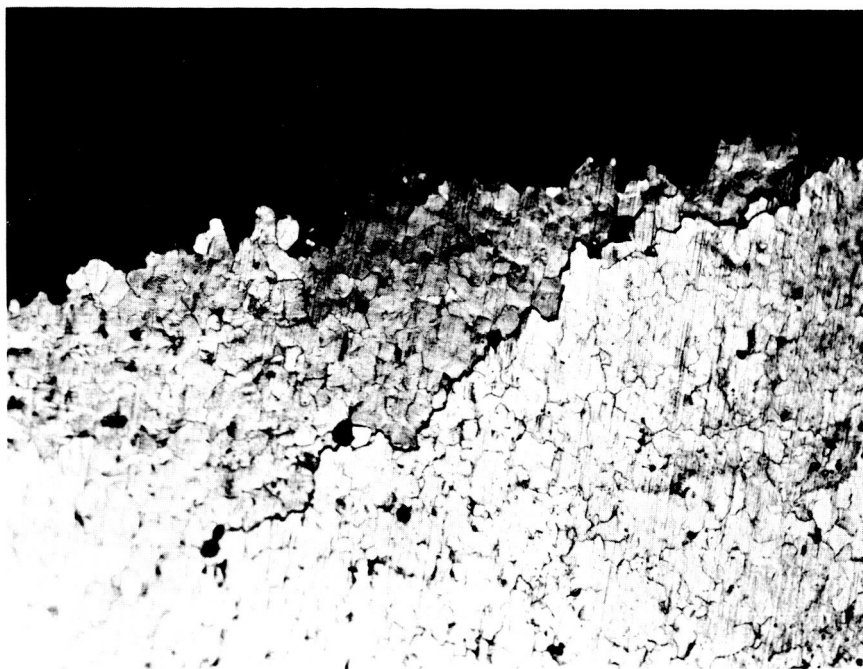
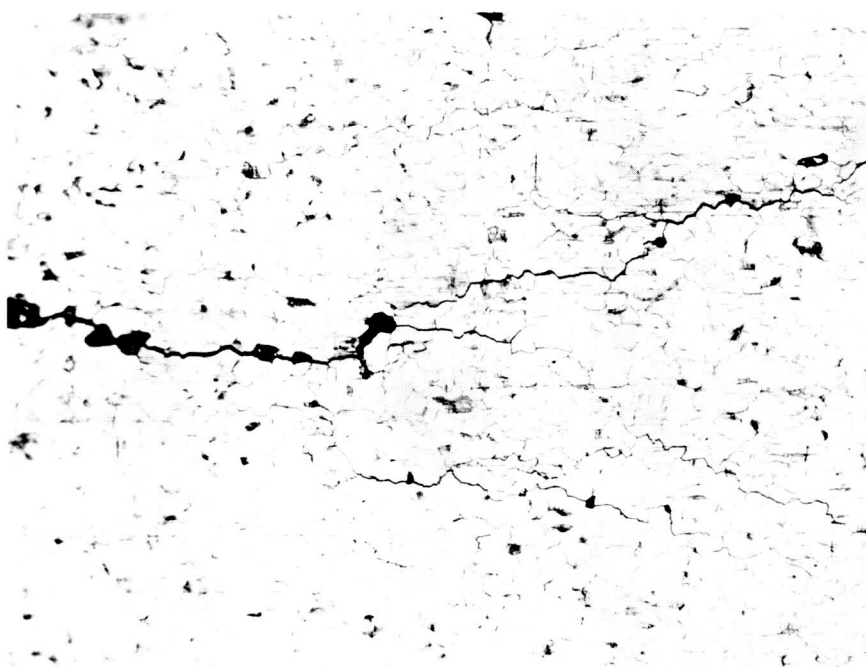


Figure 12 Deterioration of tensile properties in absence of stress.



(a)



(b)

Figure 13 Intergranular disintegration in Ti-5Al-5Sn-5Zr, after 100 hrs.  
immersion in  $\text{CH}_3\text{OH} + 0.01\text{NHCl} + 0.10\% \text{H}_2\text{O}$  without stress.  
Unetched 80X

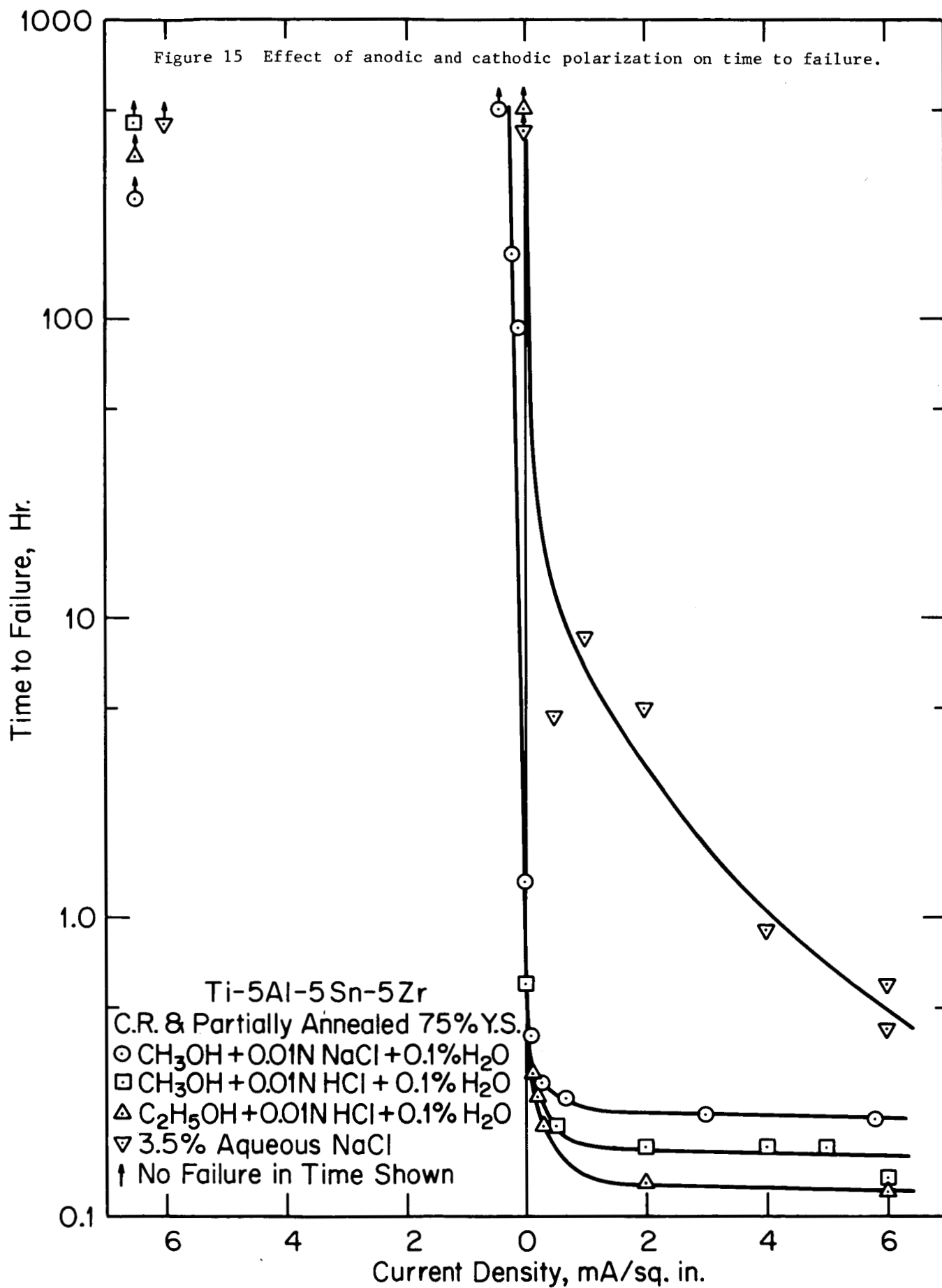


(a)



(b)

Figure 14 Intergranular "cracking" in Ti-5Al-5Sn-5Zr tensile tested in air after 6 hours immersion in  $\text{CH}_3\text{OH} + 0.01\text{NHC1} + 0.10\% \text{H}_2\text{O}$ .  
Etched 160X



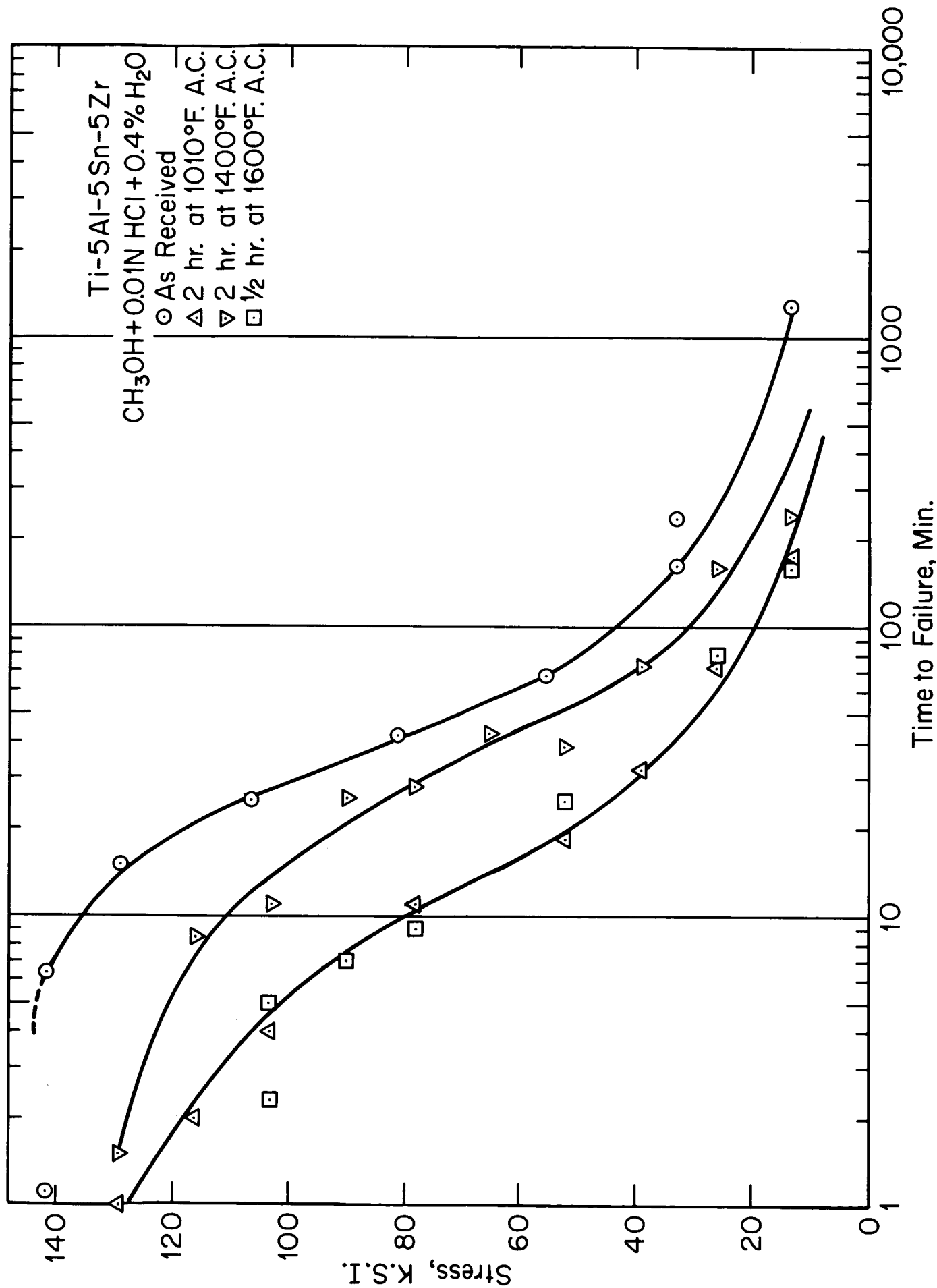


Figure 16 Effect of heat treatment and applied stress on time to failure.

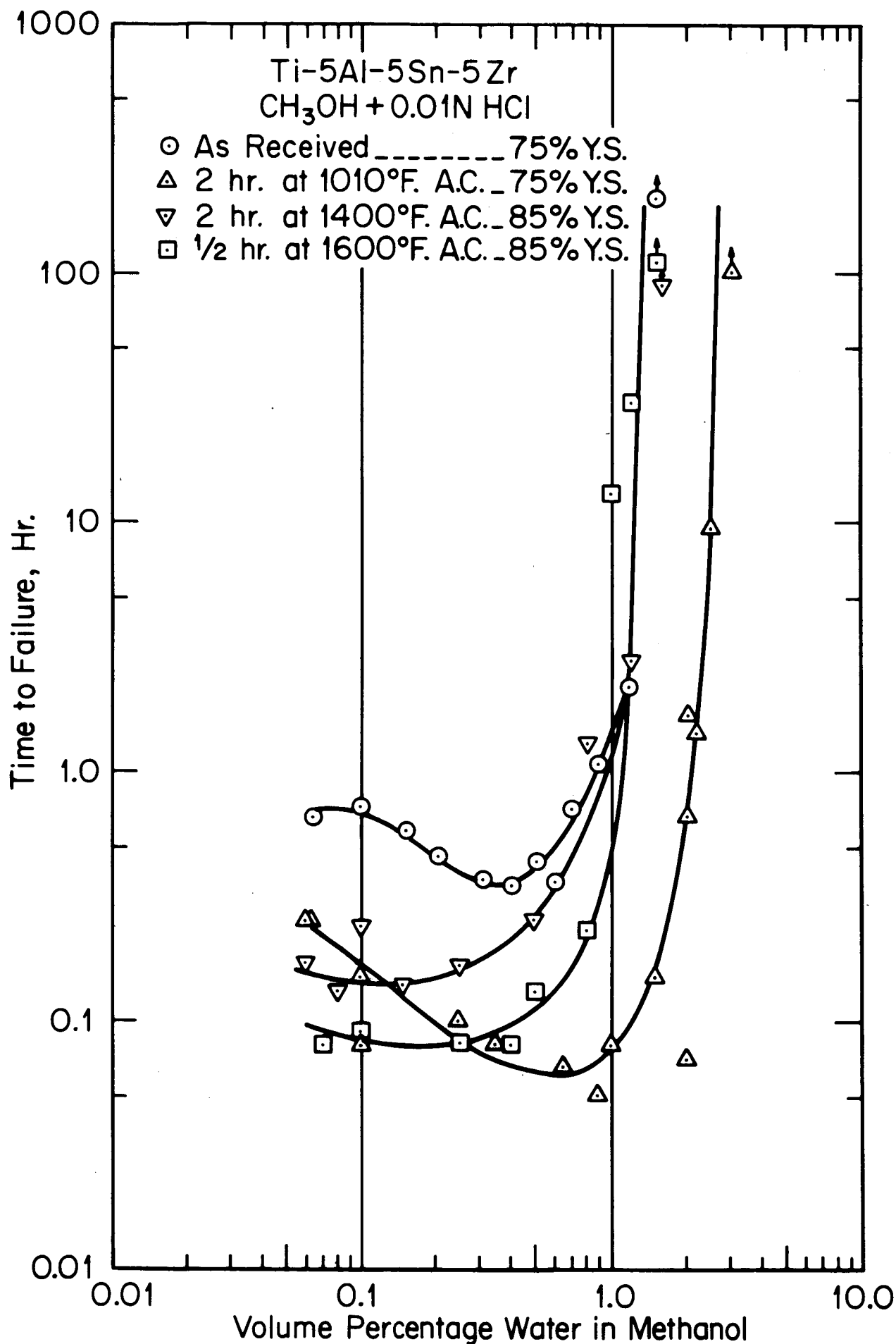


Figure 17 Effect of heat treatment and solution composition on time to failure.

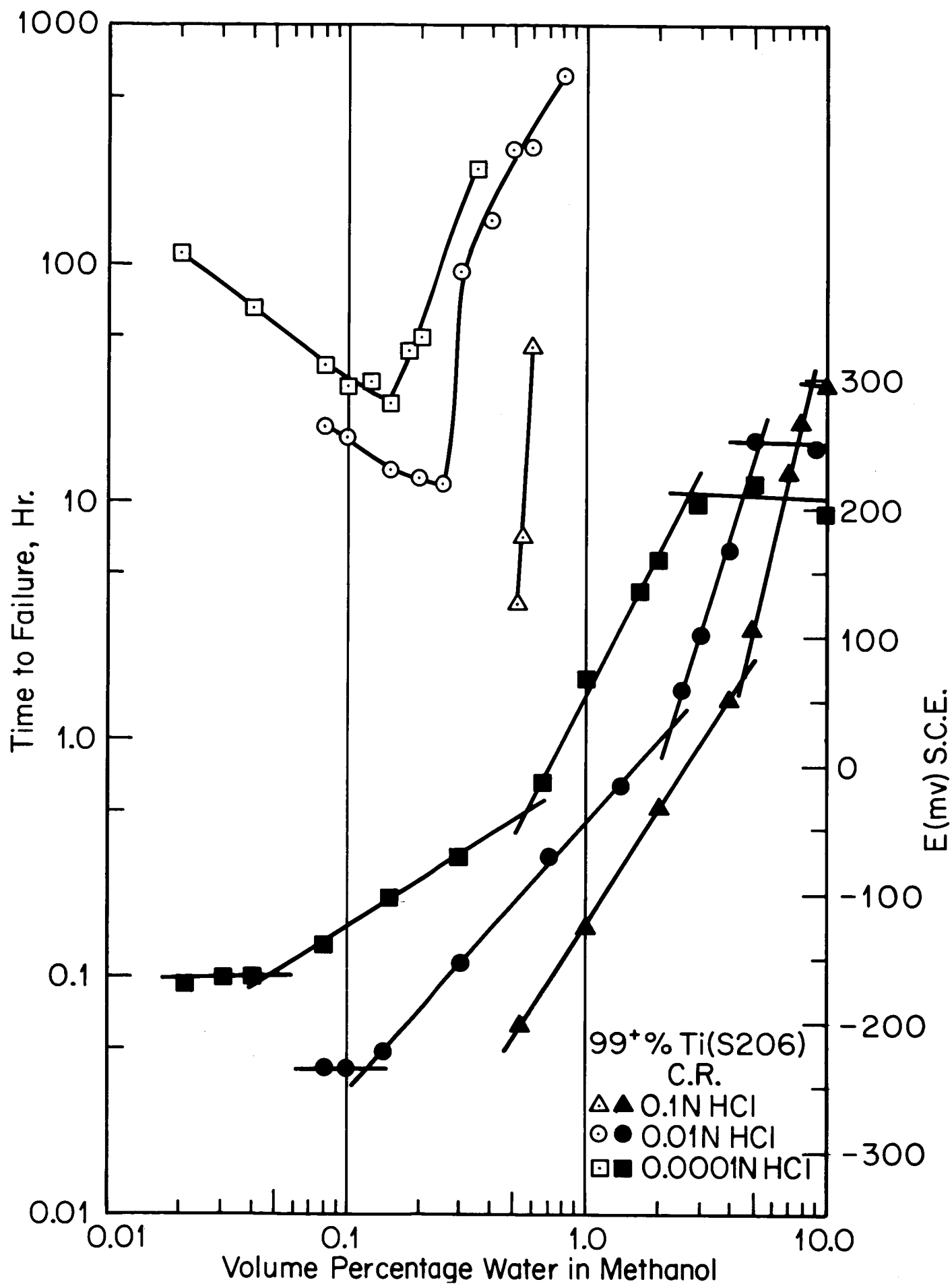


Figure 18 Comparison of time to failure with one-hour electrode potential values.

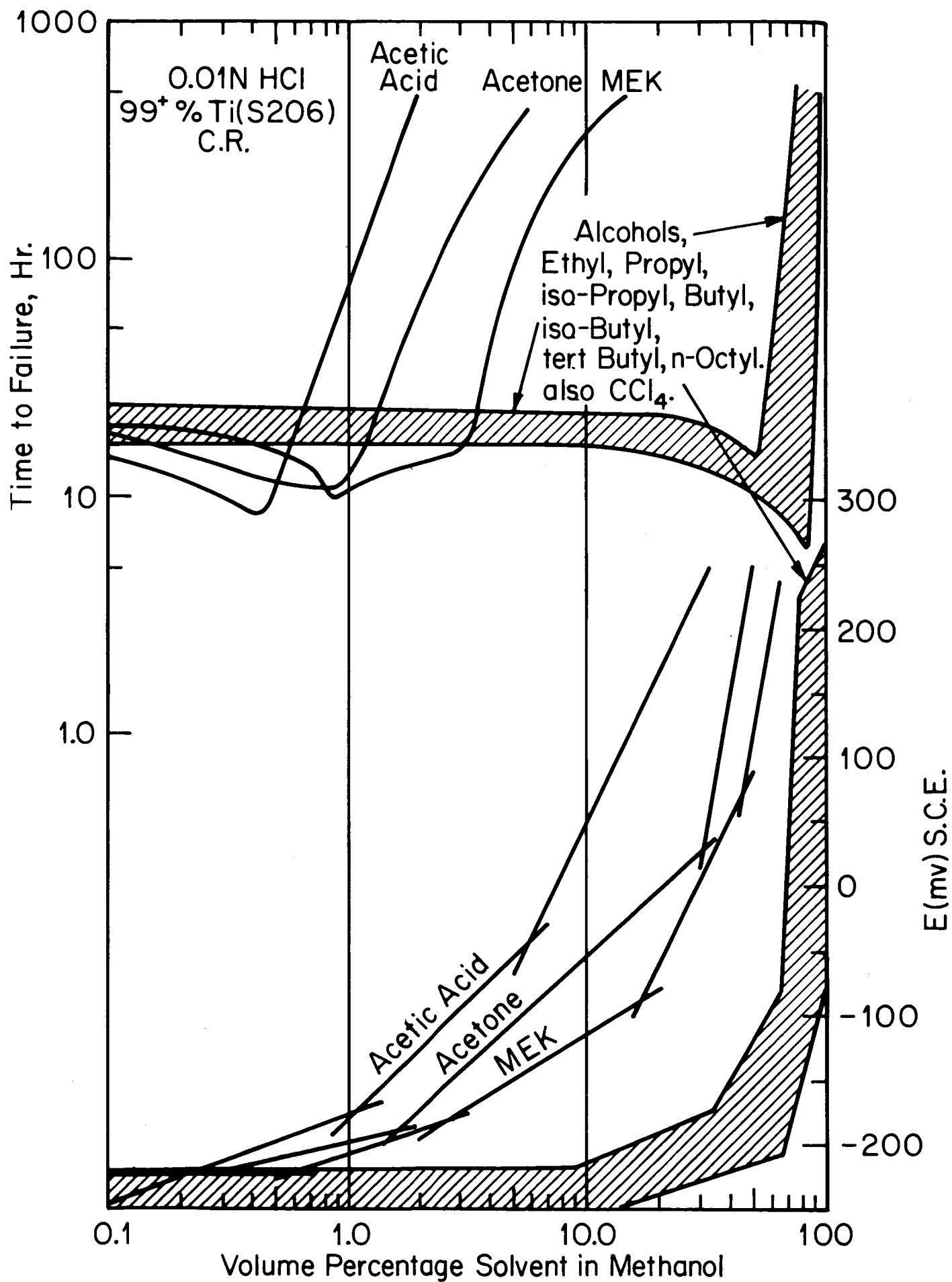


Figure 19 Comparison of time to failure with one-hour electrode potential values.

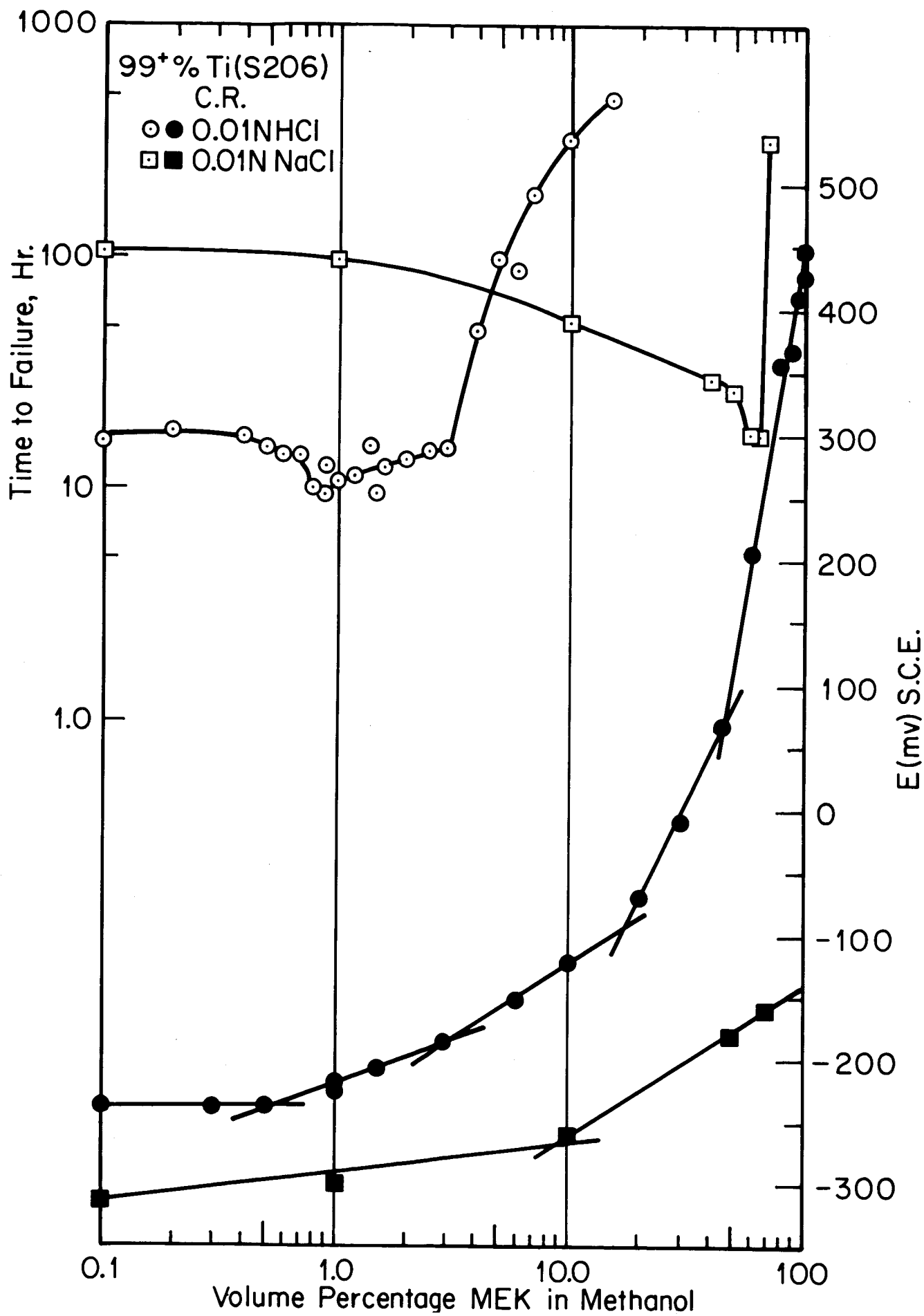


Figure 20 Comparison of time to failure with one-hour electrode potential values.

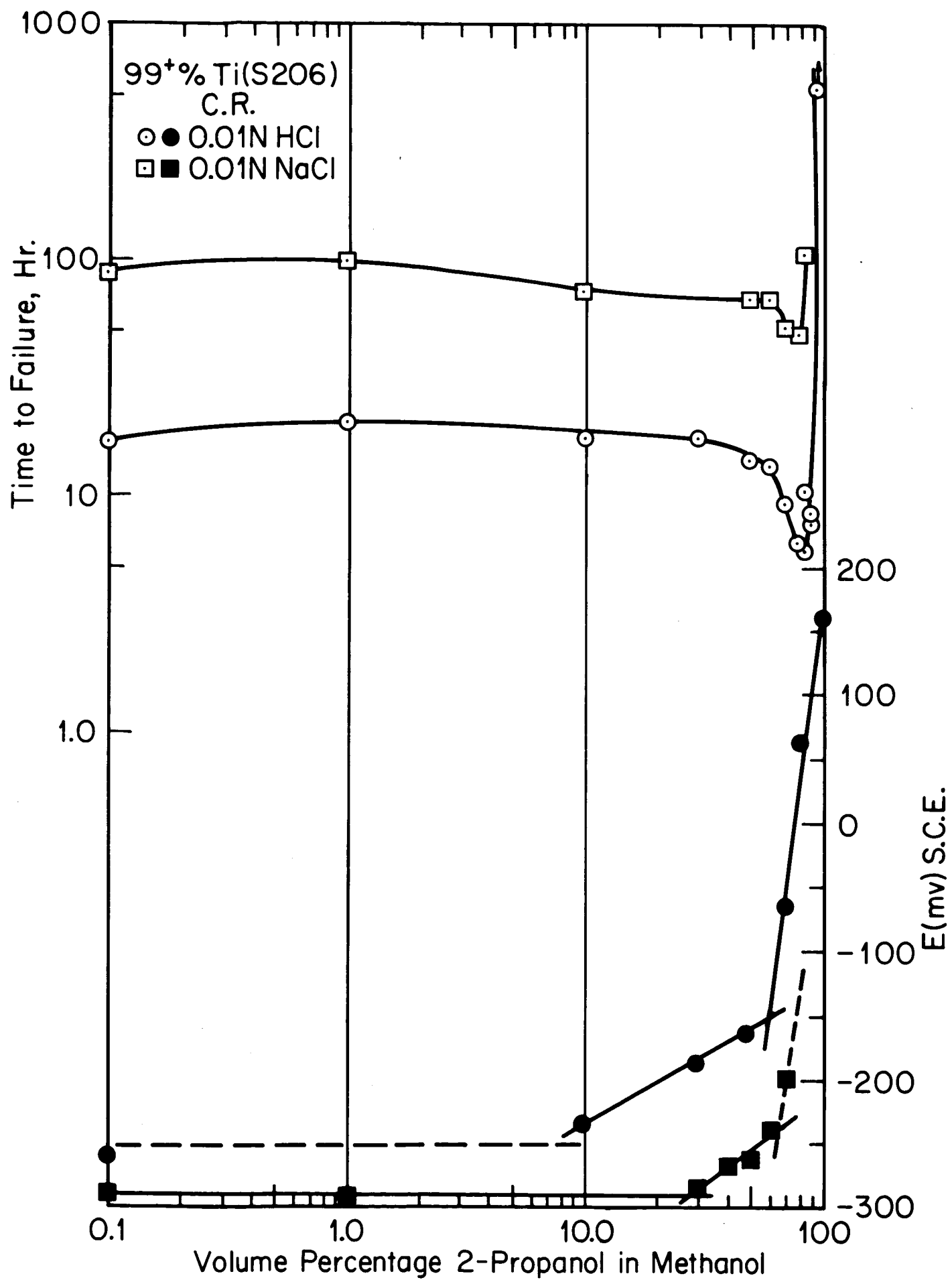


Figure 21 Comparison of time to failure with one-hour electrode potential values.

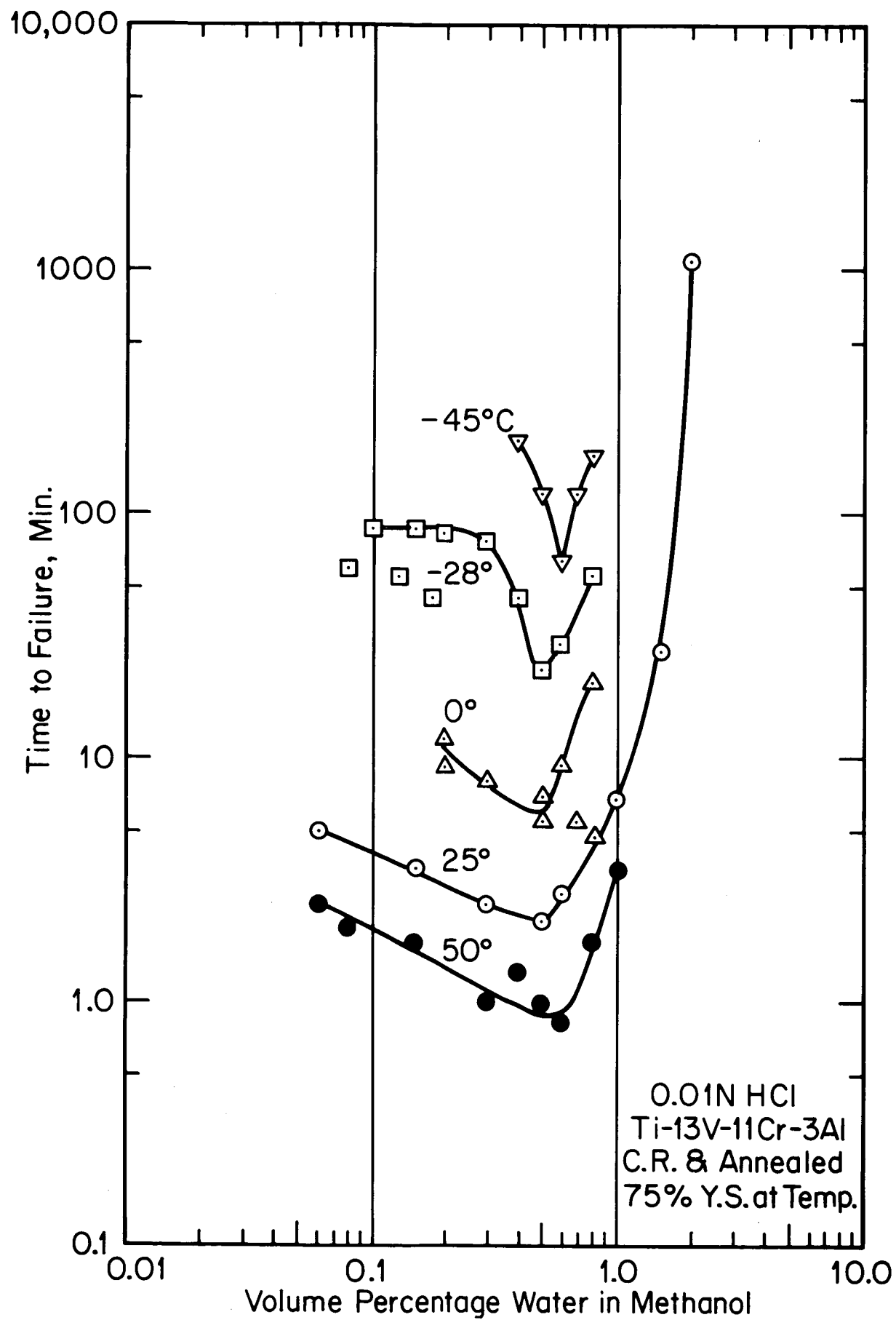


Figure 22 Effect of temperature on time to failure.

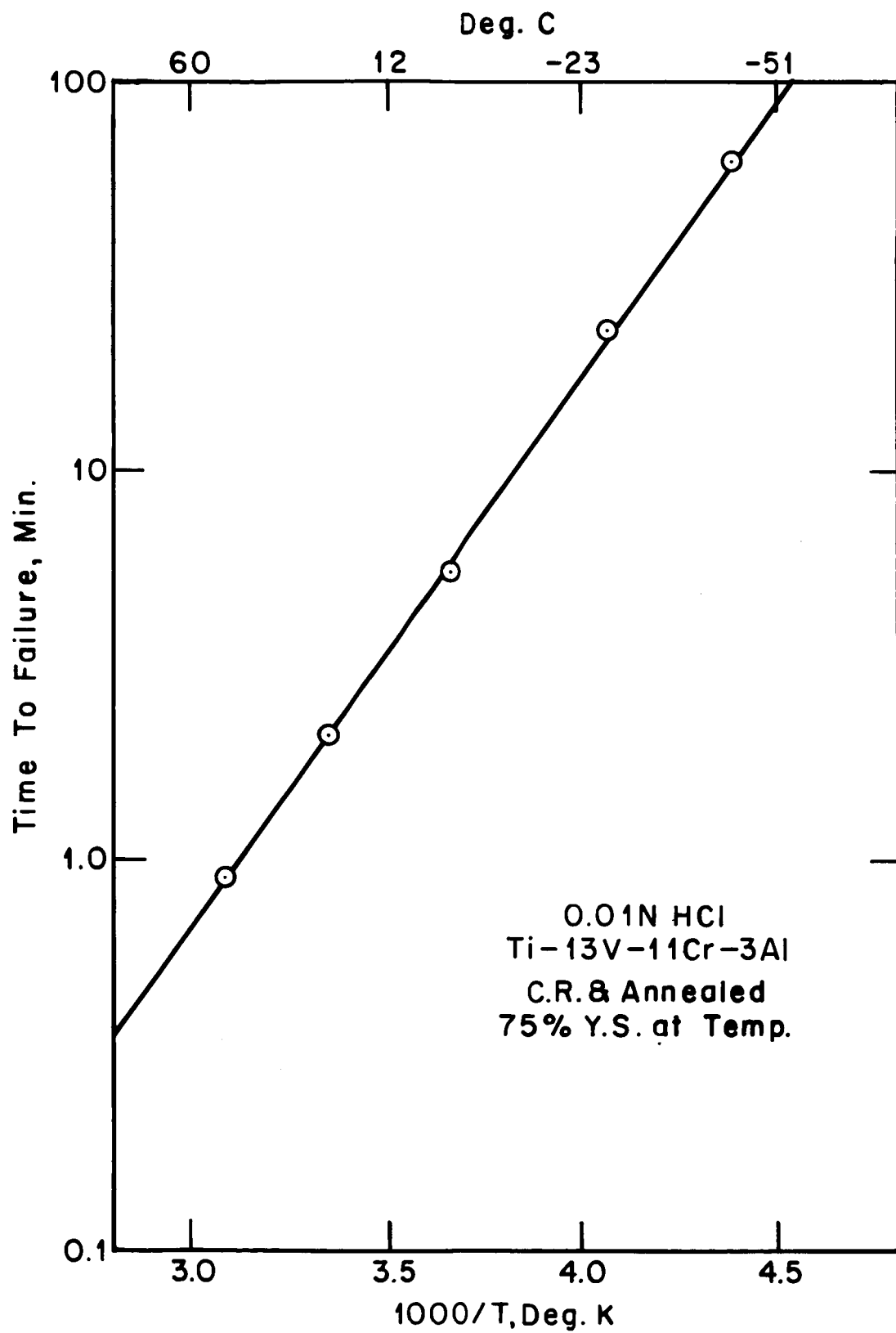


Figure 23 Effect of reciprocal temperature on minimum time to failure.